Neurochemistry International 129 (2019) 104463

Contents lists available at ScienceDirect

Neurochemistry International

journal homepage: www.elsevier.com/locate/neuint

Dopamine receptor activation mitigates mitochondrial dysfunction and oxidative stress to enhance dopaminergic neurogenesis in 6-OHDA lesioned rats: A role of Wnt signalling

Akanksha Mishra[a,d], Sonu Singh[a,b], Virendra Tiwari[a,d], Swati Chaturvedi[c,d], M. Wahajuddin[c], Shubha Shukla[a,d,*]

[a] Division of Pharmacology, CSIR-Central Drug Research Institute, Lucknow, UP, India
[b] National Institute of Child Health and Human Development, Bethesda, MD, 20814, USA
[c] Pharmaceutics & Pharmacokinetics Division, CSIR-Central Drug Research Institute, Lucknow, 226031, Uttar Pradesh, India
[d] Academy of Scientific and Innovative Research, New Delhi, India

ARTICLE INFO

Keywords:
Mitochondrial biogenesis
Adult neurogenesis
Dopamine receptors
Wnt/β-catenin signaling

ABSTRACT

Nigral dopaminergic (DAergic) cell degeneration and depletion of dopamine neurotransmitter in the midbrain are cardinal features of Parkinson's disease (PD). Dopamine system regulates different aspects of behavioural phenotypes such as motor control, reward, anxiety and depression via acting on dopamine receptors (D1-D5). Recent studies have shown the potential effects of dopamine on modulation of neurogenesis, a process of newborn neuron formation from neural stem cells (NSCs). Reduced proliferative capacity of NSCs and net neurogenesis has been reported in subventricular zone, olfactory bulb and hippocampus of patients with PD. However, the molecular and cellular mechanism of dopamine mediated modulation of DAergic neurogenesis is not defined. In this study, we attempted to investigate the molecular mechanism of dopamine receptors mediated control of DAergic neurogenesis and whether it affects mitochondrial biogenesis in 6-hydroxydopamine (6-OHDA) induced rat model of PD-like phenotypes. Unilateral administration of 6-OHDA into medial forebrain bundle potentially reduced tyrosine hydroxylase immunoreactivity, dopamine content in substantia nigra pars compacta (SNpc) and striatum region and impaired motor functions in adult rats. We found decreased D1 receptor expression, mitochondrial biogenesis, mitochondrial functions and DAergic differentiation associated with down-regulation of Wnt/β-catenin signalling in SNpc of 6-OHDA lesioned rats. Pharmacological stimulation of D1 receptor enhanced mitochondrial biogenesis, mitochondrial functions and DAergic neurogenesis that lead to improved motor functions in 6-OHDA lesioned rats. D1 agonist induced effects were attenuated following administration of D1 antagonist, whereas shRNA mediated knockdown of Axin-2, a negative regulator of Wnt signalling significantly abolished D1 antagonist induced impairment in mitochondrial biogenesis and DAergic neurogenesis in 6-OHDA lesioned rats. Our results suggest that dopamine receptor regulates DAergic neurogenesis and mitochondrial functions by activation of Wnt/β-catenin signaling in rat model of PD-like phenotypes.

1. Introduction

Parkinson's disease (PD) is the second most common age-related neurodegenerative disorder after Alzheimer's disease (AD). PD is mainly characterized by the loss of dopaminergic (DAergic) neuron in substantia nigra pars compacta (SNpc) and subsequent terminal loss of these neurons in striatum resulting in motor symptoms such as bradykinesia, rigidity, resting tremor and postural instability (Alexander, 2004). In conjugation with motor symptoms, non-motor symptoms are also commonly observed during disease progression such as anxiety, depression and cognitive impairment. Although, the pathological changes and motor dysfunctions are well reported in PD, but the precise mechanism(s) responsible for death of DAergic neurons is still unknown. Dopamine is a monoamine neurotransmitter directly implicated in motor control, reward mechanism and cognitive functions (Fowler and Benedetti, 1983). Dopamine exerts its functions via acting on

* Corresponding author. Division of Pharmacology, CSIR-Central Drug Research Institute, Sector 10, Jankipuram Extension, Sitapur Road, Lucknow, 226031, Uttar Pradesh, India.
E-mail address: shubha_shukla@cdri.res.in (S. Shukla).

https://doi.org/10.1016/j.neuint.2019.104463
Received 4 March 2019; Received in revised form 7 May 2019; Accepted 9 May 2019
Available online 10 May 2019
0197-0186/

different dopamine receptors which are commonly classified as D1-like dopamine receptor (D1 and D5) and D2-like dopamine receptor (D2, D3 and D4) (Mishra et al., 2018). Levodopa (L-Dopa) is thought to be a golden therapy for treatment of PD. However, chronic L-DOPA treatment is frequently associated with unwanted side effects including involuntary movements, akinesia, dystonia and hallucination (Mishra et al., 2018). Dopamine receptor agonists and antagonists are current therapies to delay the onset of adverse effect of L-Dopa, but they provide only symptomatic relief (Hisahara and Shimohama, 2011). D3 receptor agonist pramipexole and ropinirole has been shown to exert neuroprotective effect against MPTP and (Kitamura et al., 1997; Zou et al., 2000) and 6-OHDA (Iida et al., 1999) induced neurodegeneration. D3 receptor agonist pramipexole significantly reduced reactive oxygen species and mitochondrial dysfunction after MPP^+ toxicity in *in-vitro* as well as *in-vivo* model systems of DAergic neurodegeneration (Cassarino et al., 1998). Similarly, D2 receptor stimulation by quinpirole increased ATP synthesis, reduced ROS generation and potentially protected the striatal neurons in mouse model of PD overexpressing mutated Lrrk2 (Tozzi et al., 2018). In addition to these studies which showed the effects of dopamine agonist/antagonist on behavioural functions and DAergic neurodegeneration, several studies have also explored the effect of dopamine receptors stimulation/inhibition on birth of newborn neurons in discrete brain regions (Hedlund et al., 2016; Mishra et al., 2019; Winner et al., 2009). Formation of newborn neurons from neural progenotor cells is referred as “neurogenesis”. Neurogenesis occurs throughout mammalian life in two well defined neurogenic niches; subventricular zone (SVZ) of lateral ventricles and subgranular zone (SGZ) of hippocampal dentate gyrus (DG) (Ming and Song, 2011). Interestingly, chronic treatment with D3 receptor agonist 7-OH-DPAT increased the number of proliferating nigral bromodeoxyuridine (BrdU) expressing DAergic neuron in 6-OHDA induced rat model of PD (Van Kampen and Robertson, 2005). Winner et al. (2009) demonstrated the presence of dopamine receptors on SVZ NSCs. They also showed increased proliferation, migration and neuronal differentiation in the SVZ and olfactory bulb following chronic treatment with pramipexole to 6-OHDA induced rat model of PD (Winner et al., 2009). Similarly, D1 receptor stimulation also increases the number of proliferating $BrdU^+$ cells and formation of newborn neurons in the DG of MPTP treated mice (Zhang et al., 2016b). The magnitude of formation of newborn neurons under physiological conditions is relatively lower in the SN as compared to well defined regions such as SVZ and DG. Interestingly, whole DAergic neuronal population could be replaced by newborn cells during the lifespan of mouse, suggesting that adult neurogenesis is not limited to these two discrete neurogenic regions (Zhao et al., 2003). Lie et al. (2002) showed that the population of actively dividing progenitors produce mature glial cells not neurons in physiological conditions. Interestingly, transplantation of these freshly isolated progenitors from SN into adult hippocampus gave rise to mature neurons (Lie et al., 2002), suggesting that these progenitors possess the neurogenic potential, if exposed to appropriate environmental cues.

Mitochondrial dysfunction and oxidative damage is associated with several neurodegenerative disorder (Johri and Beal, 2012). In particular, mitochondrial dysfunction is strongly correlated with the loss of DAergic neurons in PD patient. However the molecular and cellular mechanism that control mitochondrial biogenesis in PD is not yet well defined (Schapira, 1999). The involvement and accumulation of defective mitochondria in PD has been supported by several clinical studies, showing higher level of somatic deletion of mitochondrial DNA in post-mortem brain of PD patients and aged individuals as compared to non-PD or younger controls (Kraytsberg et al., 2006; Parkinson et al., 2014). Similarly, reduced complex 1 activity and electron transfer rate and increased ROS formation have been reported in SNpc and cortex region of PD patients (Keeney et al., 2006), suggesting a series of mitochondrial dysfunction events that essentially participate in the loss of nigral DAergic neurons. The number and subcellular distribution of mitochondria in the cells are tightly regulated by mitochondrial fission and fusion process which is collectively referred as “mitochondrial biogenesis”. Several proteins are responsible for these two opposite events, such as dynamin-related protein (DRP-1) and mitochondrial fission-1 protein (Fis-1) are responsible for fission, whereas mitofusins (Mfn-1 and Mfn-2) and optic atrophy-1 (OPA-1) are responsible for fusion process. Moreover, peroxisome proliferator-activated receptor-gamma coactivator-1 alpha (PGC-1α) is a co-transcriptional regulation factor also involved in mitochondrial biogenesis and activation of different transcription factors such as nuclear respiratory factors 1 and 2 proteins (NRF-1 and NRF-2) and mitochondrial transcription factor A (TFAM) (Medeiros, 2008; Scarpulla, 2008). It has been reported that 6-OHDA induced mitochondrial fragmentation/fission involves the reduction of mitofusins and OPA-1 (mitochondrial Dynamin Like GTPase) and upregulation of Drp-1 expression in *in-vitro* and *in-vivo* models of PD (Xi et al., 2018).

Wnt/β-catenin signal transduction pathway is important for the development of central nervous system and formation of DAergic neurons in ventral midbrain. In the absence of Wnt ligands, β-catenin is marked for proteasomal degradation by “β-catenin degradation complex” which is assembled by scaffolding proteins likeAxin-2, GSK-3β, casein kinase-1 (CK-1), adenomatous polyposis coli (APC) and DVL (dishevelled) (Komiya and Habas, 2008). For the activation of intracellular signal transduction, Wnt ligand binds to Fz (Frizzled) receptors and associated co-receptors (lipoprotein receptor related proteins 5/6 (LRP5/LRP6) at cell membrane. The downstream signalling events include the association of DVL with Fz receptor, dephosphorylation of GSK-3β and inactivation of Axin-2 that leads to the dissolution of β-catenin degradation complex (Komiya and Habas, 2008). Consequently, GSK-3β is not available to phosphorylate β-catenin for degradation which thus accumulates in the cytoplasm. Therefore, hypo-phosphorylated β-catenin preferentially translocates into the nucleus where it binds with TCF/LEF transcription factor (Komiya and Habas, 2008). Growing evidence provides a link between Wnt and dopamine signaling (L'Episcopo et al., 2014; Singh et al., 2018a). In support of this notion, it has been reported that overexpression of D2 receptor inhibit Wnt signaling by acting downstream of GSK3β (Min et al., 2011). Similarly, D2 receptor agonism increases cellular level of Dvl and β-catenin in psychotic disorders (Alimohamad et al., 2005). Wnts isoforms show the functional differences in the development of ventral midbrain (VM) DAergic neurons, for example; Wnt-1 and Wnt-3a are important for specification of committed dopaminergic precursors and Wnt-5a for their terminal differentiation (Castelo-Branco et al., 2003). This study also corroborate finding on *in vivo* where disruption of Wnt1 (Andersson et al., 2008; Thomas and Capecchi, 1990), Wnt-5a or Lrp-6 (Castelo-Branco et al., 2010) genes induces the impairment in DAergic development and alter midbrain morphology. However, the precise mechanism of dopamine receptor mediated control of mitochondrial biogenesis and formation of new dopaminergic neurons in PD is not defined. In the present study, we show that D1 receptor signalling via Wnt/β-catenin signalling pathway improve mitochondrial biogenesis and maintain DAergic neurogenesis in 6-OHDA induced rat model of PD-like phenotypes.

2. Material and methods

2.1. Animals

Adult male Sprague Dawley (SD) rat were obtained from National Laboratory Animal Centre (NLAC) of Central Drug Research Institute, Lucknow, India. Rats were maintained under standard laboratory conditions with a 12-h–light/–dark cycle and ad libitum access to food and water during the study. The animal experiment protocol and experimental procedure was carried out in accordance to Institutional Animals Ethics Committee (IAEC) following the guidelines of CPCSEA (Committee for the Purpose of Control and Supervision of Experiment on Animals), which complies with international norms of INSA (Indian National Science Academy).

2.2. 6-OHDA lessoning

6-OHDA lessoning was performed according to our previous study (Singh et al., 2018a). In brief, rats were injected with desipramine (25 mg/kg/i.p; Sigma-Aldrich, St. Louis, MO, USA), a noradrenergic reuptake inhibitor. After 30 min of desipramine, rats were anesthetized with sodium pentobarbital (40 mg/kg, i. p) and placed in a stereotaxic frame. Total 16 μg of 6-OHDA-hydrobromide (8 μg/μl; in normal saline containing 0.02% ascorbic acid) was unilaterally injected into the right medial forebrain bundle (MFB) at a rate of 0.5 μl/min at the following stereotaxic coordinates related to Bregma; AP = −4.4, ML = 1.2, DV = - 7.8 mm using 30-gauge Hamilton syringe. The needle was placed in for an additional 5 min before being retracted to prevent backflow.

2.3. Lentiviral vector administration

To determine the role of Wnt/β-catenin signalling in mitochondrial biogenesis and DAergic neurogenesis in rat model of PD. Axin-2 shRNA lentivirus particles were stereotaxically injected in the right SNpc of rats according to our previous study (Singh et al., 2018a). Ready to use pLKO.1-puro-CMV-tGFP Mission® lentivirus particles were procured from Sigma Aldrich (St. Louis, USA). The Axin-2 knockdown targeting sequence was 5′-AAAGGGAAATTACAGGTATTA-3′ and nontargeted or scrambled (sc) shRNA (Sigma Aldrich, St. Louis, USA) was used as a control. Lentiviral particles were injected at the same time of 6-OHDA injection. Green fluorescent protein (GFP) tagged Axin-2 shRNA lentivirus particles (2.1×10^7 TU/ml) were injected with a 10-μl Hamilton syringe at a speed of 0.2 μl/min at the following anterior-posterior, lateral and ventral coordinates related to Bregma, AP = −5.2, ML = 2.5, DV = - 7.6 mm. At the end of injection, needle was left in place for an additional 5 min before being retracted.

2.4. Drugs and treatment

Drug administration protocol was divided into two set of experiment. In the first experiment, rats were divided into seven groups. All drug treatment started 3 days prior to 6-OHDA injection and continued for another 21 days from day of 6-OHDA injection.

2.4.1. Control group
Received 2 μl of saline stereotaxically in right MFB.

2.4.2. 6-OHDA lesioned group
Received 2 μl of 6-OHDA (8 μg/μl) saline in right MFB.

2.4.3. 6-OHDA + SKF-38393 group
Rats were injected with D1 receptor agonist SKF-38393 (10 mg/kg, i. p, Sigma Aldrich, USA).

2.4.4. 6-OHDA + SKF-38393 + SCH- 23390 group
6-OHDA + SKF-38393 treated rats were received D1 antagonist SCH-23390 (0.5 mg/kg, i. p, Sigma Aldrich, USA).

2.4.5. 6-OHDA + Bromocriptine group
6-OHDA lesioned rats received D2 receptor agonist bromocriptine (0.2 mg/kg, i. p, Sigma Aldrich, USA).

2.4.6. 6-OHDA + Bromocriptine + raclopride group
6-OHDA + bromocriptine treated rats were received D2 receptor antagonist raclopride (5 mg/kg, i. p, Sigma Aldrich, USA).

2.4.7. 6-OHDA + L-DOPA group
6-OHDA lesioned rats received L-DOPA (25 mg/kg, i. p) + benesrazide (15 mg/kg, i. p).

In the second experiment, animals were divided into four groups. All drug treatment started 3 days prior to 6-OHDA injection and continued for another 21 days from day of 6-OHDA injection.

2.4.2.1. ScshRNA group (control). Rats stereotaxically received 2 μl of scrambled (sc) shRNA lentivirus particles into SNpc.

2.4.2.2. 6-OHDA + ScshRNA. Rats were stereotaxically received 2 μl of 6-OHDA (8 μg/μl) into right MFB along with 2 μl of scshRNA lentivirus particles into SNpc. ScshRNA was injected at the same time of 6-OHDA injection.

2.4.2.3. 6-OHDA + ScshRNA + S KF-38393 + SCH-23390. 6-OHDA + scshRNA treated rats were cotreated with D1 agonist SKF-38393 followed by D1 antagonist SCH-23390.

2.4.2.4. 6-OHDA + Axin-2 shRNA + SKF-38383 + SCH-23390. 6-OHDA lesioned rats were received Axin-2 shRNA (2 μl) into SNpc at the same time of 6-OHDA injection. 6-OHDA + Axin-2 shRNA injected rats were cotreated with D1 agonist SKF-38393 followed by D1 antagonist SCH-23390. Drug doses were selected according to the effective doses reported in previous rodent studies (Mishra et al., 2019).

2.5. Bromodeoxyuridine (BrdU) administration

To investigate the effect of dopamine receptors modulation and Axin-2 knockdown on DAergic neurogenesis in 6-OHDA treated rats, BrdU was injected (50 mg/kg, i. p.) daily for 3 days starting from the next day of 6-OHDA injection. BrdU is a thymidine analogue that specifically label cells during S-phase, therefore, used as a proliferation marker.

2.6. Open-field activity test

The locomotor activity was measured on day 21 post 6-OHDA injection by Optovarimax (OptoM-3, Columbus Instruments, USA) as previously described (Singh et al., 2017, 2018a). In brief, rats were placed in an open field arena (45 cm × 45 cm) surrounded by plexiglass walls in a quiet and sound proof room. Rats were acclimatized for 10 min in open-field arena prior to start experiment. The activity was monitored over a period of 30 min. At the end of experiment, rats were removed from the open field, and the experimental chamber was thoroughly cleaned with 70% alcohol to avoid the interference odour of previous rat.

2.7. Rotarod test

Balance and neuromuscular coordination was measured by rotarod apparatus (Rotamax-5, Columbus Instruments, USA) under an accelerating protocol previously described (Singh et al., 2018a). Rats were pre-trained on rotating rod for 3–4 days prior to 6-OHDA lesioned to verify that they could maintain themselves on rotating rod for 300 s. On day 21 post-6-OHDA injection latency to fall from rotating rod was recorded using the same protocol.

2.8. Amphetamine-induced circling behaviour

Amphetamine (5 mg/kg, i. p.) induced ipsilateral rotations analysis was performed on day 21 post-6-OHDA injection to evaluate the effect of dopamine receptor agonist and antagonist on lesion severity. 30 min after amphetamine administration, rotational behaviour was monitored for periods of 30 min as describe earlier published method (Singh et al., 2018a). The data is expressed as net ipsilateral rotations per 30 min (net ipsilateral rotations = ipsilateral rotations in 30 min-contralateral rotations in 30 min).

2.9. High performance liquid chromatography (HPLC)

Briefly, brain part such as striatum and SNpc was homogenised in ice cold Tris-EDTA buffer, pH 7.4 at a ratio of 1:2. A simple protein precipitation technique was used for extraction of the compounds from tissue using acetonitrile as an extracting solvent. To 50 µL of homogenised tissue, 100 µL of acetonitrile was added and vortexed for 10 min followed by centrifugation 10 min at 12,000 rpm on Sigma 3–16 K (Frankfurt, Germany). 80 µl of organic layer was separated and 20 µL was injected into the analytical column for detection. The concentration of Dopamine was analyzed using Shimadzu HPLC system (Kyoto, Japan) equipped with a LC-10 ATVP pump, DGU-14A degasser, SCL-10 AVP system controller, SIL-10 ADVP injector and a SPD-M10 AVP photo diode array detector. Separation of dopamine was done on Supelco Discovery Cyano C_{18} column (15 mm × 4.6 mm, 5.0 µm)using mobile phase: acetonitrile (acidified with 0.1% formic acid): 0.1% formic acid in the ratio of 70:30 (v/v) at a flow rate of 0.5 mL/min for dopamine. The detection wavelength was 258 nm for dopamine.

2.10. Total ATP measurement

Total ATP was measured using commercially available ATP Colorimetric assay kits (BioVision, CA, USA). Tissues were homogenised in ATP assay buffer, centrifuged at 18,000 × *g* for 10 min at 4^0C and supernatant was used for ATP and protein measurement. Absorbance was measured at 570 nm using an ELISA plate reader (BioTek Instruments, USA) and the result expressed as µmol/g of tissue weight.

2.11. Citrate synthase activity

Citrate synthase activity in brain tissues were measured using a commercially available enzyme assay kit (Biovision, CA, USA) according to the manufacturer's instructions. Tissues were homogenised in assay buffer provided with kit, centrifuged at 10,000 × *g* for 5 min at 4 °C and supernatant was used for citrate synthase activity and protein measurement. Citrate synthase activity was measured at 412 nm in kinetic mode at 25 °C for 20–40 min, normalized by GSH standard and expressed in nmol/min/µl.

2.12. Flow cytometry analysis

Mitochondrial membrane potential (ΨM, MMP) was assessed using mitochondrial membrane potential sensitive carbocyanine dye JC-1 (5,5′,6,6′-tetrachloro-1,1′,3,3′-tetraethyl-benzamidazolocarbocyanine iodide, Sigma Aldrich, USA) in SNpc as described in our previous publication (Singh et al., 2018a). Intact mitochondria were isolated from freshly dissected tissues using a mitochondria isolation kit (Qiazen, Hilden, Germany) following manufacturer's instructions. Mitochondrial protein concentrations was measured by BCA protein assay kit (Thermo Scientific, USA) and total 5 µg of mitochondria used for FACS analysis. Freshly isolated mitochondria were stained with fluorescent probe JC-1 (Sigma Aldrich, USA) at 2.5 µg/ml and incubated for 20 min at 37 °C. Total 10,000 events were acquired and analyzed by FACS Calibur.

2.13. Western blotting

Brain tissues (SNpc) were lysed in NE-PER reagent (Pierce/Thermo Fisher Scientific, USA) supplemented with protease inhibitor cocktail (Sigma Aldrich, St. Louis, USA) to extract nuclear and cytosolic fraction of protein. Total protein concentration was measured using the BCA protein assay kit (Pierce/Thermo Fisher, USA). Western blotting was then carried out as previously described (Reddy et al., 2018; Singh et al., 2017, 2018a). Cytosolic fraction and nuclear fraction were denatured in protein loading buffer supplemented with 5% β-Marceptoethanol at 95 °C for 5 min. Protein samples analysed for dopamine receptor expression analysis were not boiled in lysis buffer. Total 30 µg proteins were separated onto 10% SDS-polyacrylamide gel. After electrophoresis, the gels were transferred onto the PVDF (polyvinyl difluoride) membranes. The PVDF membrane was blocked with 5% non-fat dry milk in Tris-buffered saline containing 0.1% Tween-20 followed by incubation at 4^0C for overnight with primary antibody against mouse anti- GSK-3β (1:1000, Thermo Scientific, IL, USA), mouse anti-pTyr216-GSK-3β (1:1000, Millipore, Temecula, CA, USA), rabbit anti-p-β-catenin (1:500, Thermo Scientific, USA), mouse anti-APC (1:1000, Abcam, Cambridge, UK), rabbit anti- Axin-2 (1:1000, Abcam, Cambridge, UK), rabbit anti- β-catenin (1:5000, Abcam, Cambridge, UK), rabbit anti- TFAM (1:1000, Merck Millipore, USA), rabbit anti- Mfn-2 (1:1000, Merck Millipore, USA), rabbit anti- Fis-1 (Thermo Scientific, USA), mouse anti-OPA-1 (1:2000, Thermo Scientific, USA), rabbit anti-DRP-1 (1:1000, Merck Millipore, USA), rabbit anti-histone H3 (1:500, Sigma), mouse anti- β-actin (1:2000, Sigma). After overnight incubation, membranes were washed three times with TBST and incubated for 2 h at room temperature with horseradish peroxidase (HRP) conjugated secondary antibody: goat anti-rabbit IgG or rabbit anti-mouse IgG (1:3000, Sigma Aldrich, St Louis, USA). Images were visualized using enhanced chemiluminescent (ECL) substrate kit (Thermo Pierce, USA) was immunoreactivity was quantified by myImage analysis software (Thermo scientific, USA**).**

2.14. Immunohistochemistry

Immunohistochemistry was performed as our previously described methods (Singh et al., 2017, 2018a). In brief, rats were deeply anesthetized with sodium pentobarbital (40 mg/kg, i. p) and transcardially perfused with PBS following ice-cold 4% (w/v) paraformaldehyde (PFA) in 0.1 M sodium phosphate buffer (PBS, pH 7.5). The brain were dissected and post fixed in the same fixative over night at 4 °C and transferred into 30% sucrose solution for cryoprotection. 30 µm thick coronal sections were cut using cryostat (Thermo Scientific, USA) as previously described (Singh et al., 2018a, 2018b) and every 5th serial section encompassing SNpc or striatum was collected for immunohistochemistry analysis. Coronal section were washed three times with TBS and permeabilized with TBS containing 0.2% Triton X-100 (TBST) for 30 min at room temperature. After permeabilization, section were blocked with 5% BSA in TBST for 2 h at room temperature then section was incubated with primary antibody against rabbit anti-tyrosine hydroxylase (TH, 1:1000, Merck Millipore, CA, USA), Guinea pig anti- Doublecortin (DCX) (DCX, 1:1000, Merck Millipore, CA, USA), mouse anti-tyrosine hydroxylase (TH, 1:1000, Merck Millipore, CA, USA) and rabbit anti-COXIV (1:500, Merck Millipore, CA, USA) for overnight at 4 °C.

2.15. BrdU staining

BrdU staining was performed as previously describe method (Singh et al., 2017, 2018b). Permeabilized sections were treated with 1N-HCl for 10 min at 4 °C followed by in 2N-HCl for 20 min at 37 °C to denature the DNA. After denaturation, the sections were incubated in borate buffer (0.1 M, pH- 8.5) to neutralize the acidic medium. Section were rinsed three times with TBS, and blocked with 5% BSA in TBST for 2 h at room temperature. After blocking, section were incubated in primary antibodies against, rabbit anti- TH (1:1000, Merck Millipore, CA, USA) and mouse anti- BrdU (1:200, Merck Millipore, CA, USA) at 4 °C for overnight. After washing, sections were incubated with appropriate Alexa fluor- 488/594 conjugated secondary antibodies (Molecular Probes, Eugene, USA) for 2 h in dark at room temperature. Sections were mounted on glass slide with Fluoroshield DAPI mounting medium (Sigma Aldrich, USA) and analyzed by Leica inverted fluorescent microscope equipped with a digital CCD camera (Leica, Watzlar, Germany) using 10x or 20x objective. Immuno positive cells were

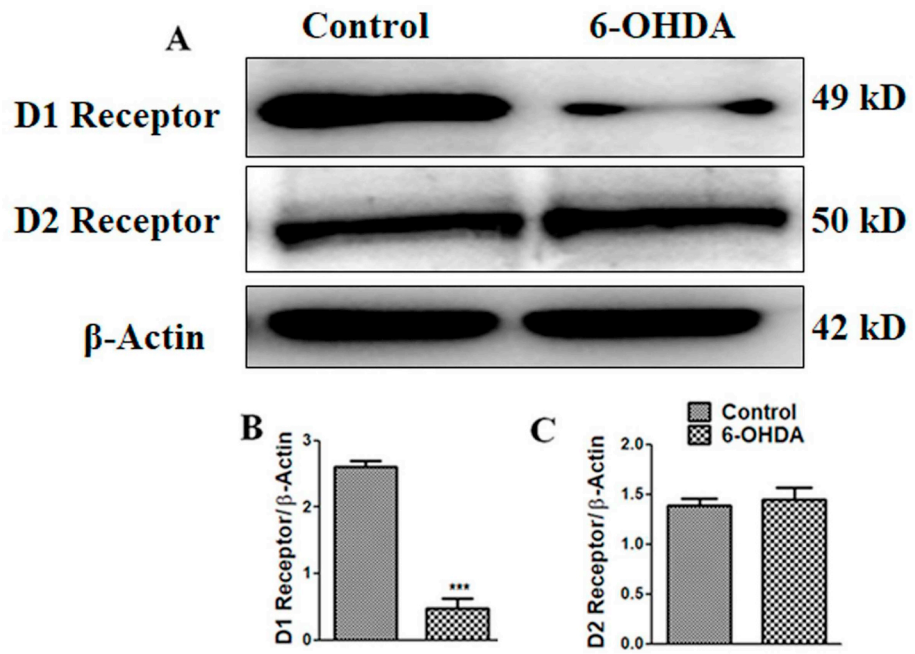

Fig. 1. 6-OHDA administration decreases D1 receptor expression in SNpc region in 6-OHDA induced rat model of PD. (A) Representative immunoblots shows expression of D1 receptor and D2 receptor in the SNpc. Bar graphs show the quantification of **(B)** D1 receptor, **(C)** D2 receptor relative protein density in the SNpc. The protein density of D1 and D2 receptor was normalized with β-actin. Data are expressed as mean ± SEM of n = 5 rats/group. Data were analyzed by student t - test (***P < 0.001) * = Control vs 6-OHDA.

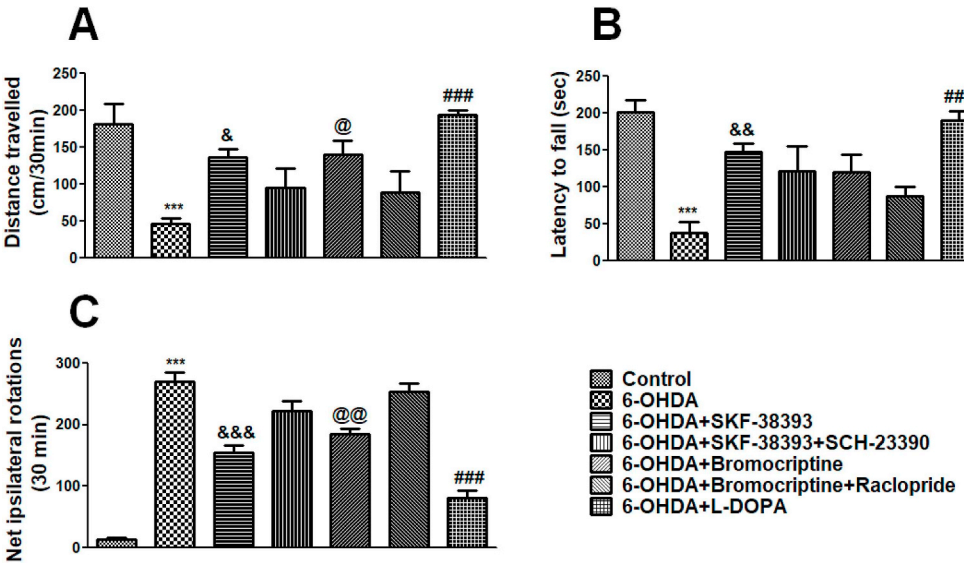

Fig. 2. D1 receptor activation attenuates 6-OHDA induced behavioural impairment in 6-OHDA induced rat model of PD. Figure A–C shows effect of D1 and D2 receptor agonist and antagonist on behavioural function in 6-OHDA lesioned rats. **(A)** Bar graph shows spontaneous locomotor activity, represented as distance travelled over a 30-min period. **(B)** Bar graph shows the performance on rotarod, evaluated as latency to fall from the rod, for a period of 300 s. **(C)** Bar graph shows Amphetamine (5 mg/kg, i. p.) induced net ipsilateral rotations, observed over a period of 30 min. Data are expressed as mean ± SEM of n = 8 rats/group. Data were analyzed by One-way ANOVA followed by Bonferroni's Multiple Comparison Test (*P < 0.05, **P < 0.01, ***P < 0.001, $^{\&}$P < 0.05, $^{\&\&}$P < 0.01, $^{\&\&\&}$P < 0.001 $^{@}$P < 0.05, $^{@@}$P < 0.01, $^{@@@}$P < 0.001, $^{\#}$P < 0.05, $^{\#\#}$P < 0.01, $^{\#\#\#}$P < 0.001) * = Control vs 6-OHDA, & = 6-OHDA vs 6-OHDA + SKF-38393, @ = 6-OHDA vs 6-OHDA + Bromocriptine, # = 6-OHDA vs 6-OHDA + L-DOPA.

quantified by ImageJ software (NIH) following our previous published method (Singh et al., 2018a).

2.16. Statistical analysis

All statistical analysis was done by GraphPad Prism software 5.00 (San Diego, CA, USA) and data are expressed as means ± standard error of mean (SEM), and difference between the groups was determined using one-way analysis of variance (ANOVA) followed by Bonferroni post-hoc test and *t*-test. The difference between the groups was considered to be statistically significant when "p" values were less than 0.05.

3. Results

3.1. 6-OHDA reduces dopamine receptor D1 levels in SNpc region

To investigate the effect of unilateral injection of 6-OHDA on dopamine receptors (DR) levels, we measured protein levels of dopamine receptor DRD1 and DRD2 in the SNpc (Fig. 1A). We found that the level of D1 receptor level was significantly down-regulated in the SNpc of 6-OHDA lesioned rats as compared control rats (Fig. 1B, P < 0.001). In contrast, D2 receptor level was not significantly altered in SNpc region of 6-OHDA lesioned rats (Fig. 1C, P > 0.05).

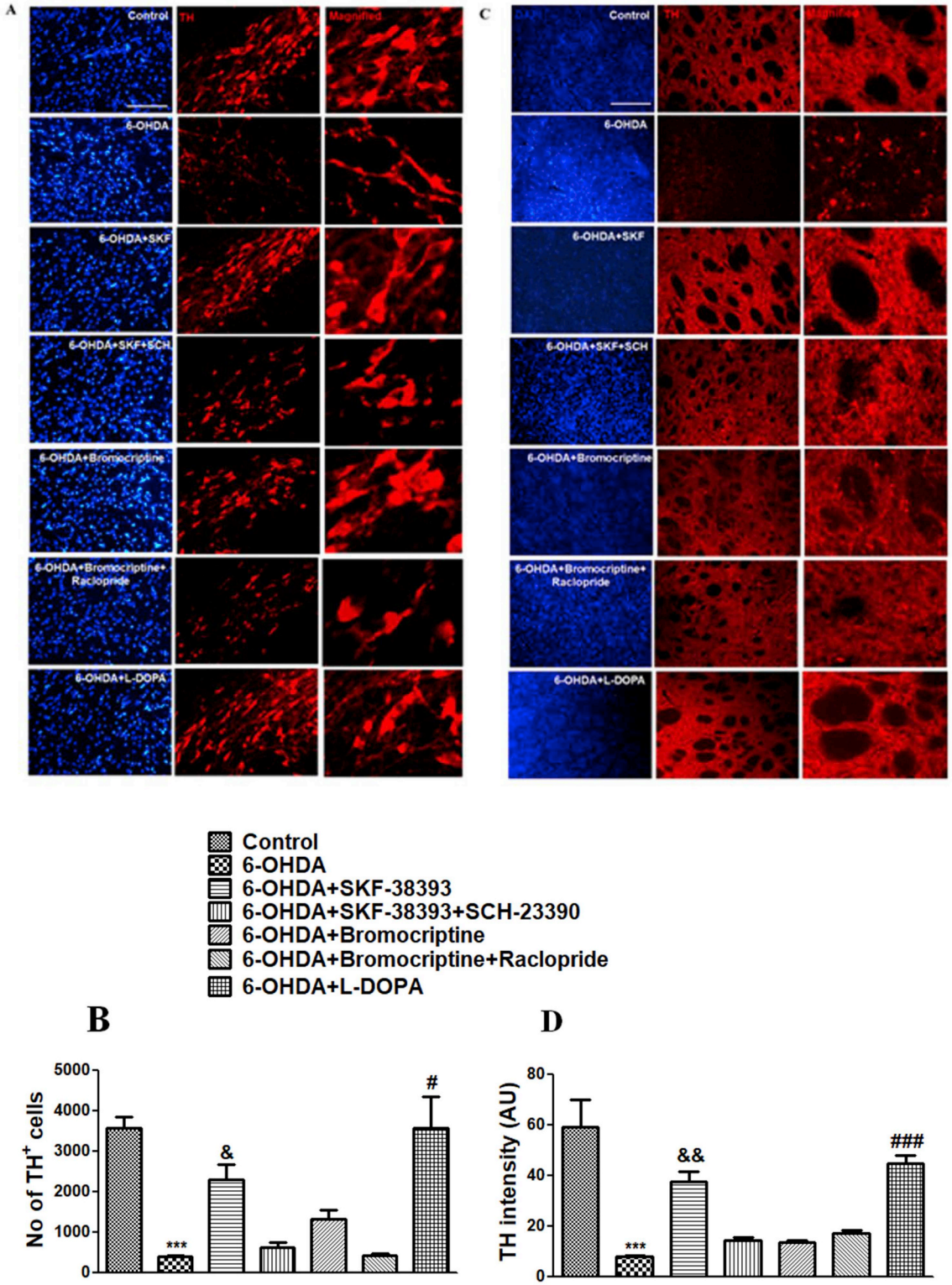

Fig. 3. D1 receptor stimulation enhances dopaminergic neuronal population and their terminals in 6-OHDA induced rat model of PD, **(A and C)** Representative photomicrographs show immunostaining of tyrosine hydroxylase (TH) in the SNpc and striatum region. Scale bar = 50 μm for all photomicrographs. **(B)** Bar graph shows quantitative analysis of TH + DAergic cells in the SNpc region. **(D)** Bar graph shows average intensity of TH immunoreactive axon fibres in the striatum region. Data are expressed as mean ± SEM of n = 4 rats/group. Data were analyzed by One-way ANOVA followed by Bonferroni's Multiple Comparison Test ($^{*}P < 0.05$, $^{**}P < 0.01$, $^{***}P < 0.001$, $^{\&}P < 0.05$, $^{\&\&}P < 0.01$,$^{\&\&\&}P < 0.001$ $^{@}P < 0.05$, $^{@@}P < 0.01$,$^{@@@}P < 0.001$, $^{\#}P < 0.05$, $^{\#\#}P < 0.01$, $^{\#\#\#}P < 0.001$) * = Control vs 6-OHDA, & = 6-OHDA vs 6-OHDA + SKF-38393, @ = 6-OHDA vs 6-OHDA + Bromocriptine, # = 6-OHDA vs 6-OHDA + L-DOPA.

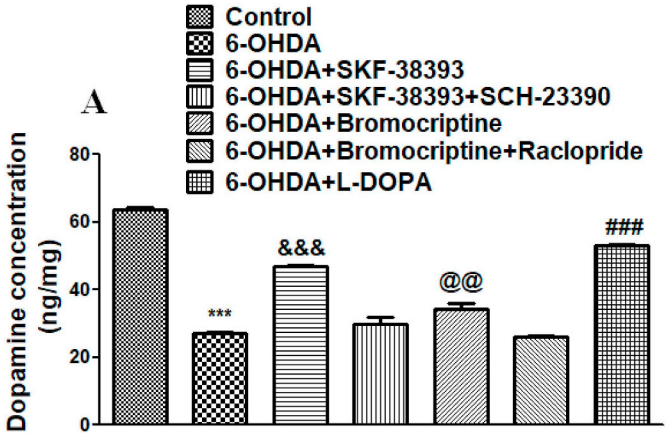

Fig. 4. D1 receptor activation increases dopamine level in 6-OHDA induced rat model of PD. **(A)** Bar graph shows concentration of dopamine level in striatum region. Data were analyzed by One-way ANOVA followed by Bonferroni's Multiple Comparison Test (*P < 0.05, **P < 0.01, ***P < 0.001, $^{\&}$P < 0.05, $^{\&\&}$P < 0.01,$^{\&\&\&}$P < 0.001 $^{@}$P < 0.05, $^{@@}$P < 0.01,$^{@@@}$P < 0.001, $^{\#}$P < 0.05, $^{\#\#}$P < 0.01, $^{\#\#\#}$P < 0.001) * = Control vs 6-OHDA, & = 6-OHDA vs 6-OHDA + SKF-38393, @ = 6-OHDA vs 6-OHDA + Bromocriptine, # = 6-OHDA vs 6-OHDA + L-DOPA.

3.2. D1 receptor agonism attenuates 6-OHDA induced behavioural deficits in rat model of PD-like phenotypes

We (Singh et al., 2017, 2018a, 2018b) and others (Carvalho et al., 2013) have previously reported that single unilateral injection of 6-OHDA into MFB induce behavioural deficits in rats. Therefore, we were interested to determine whether administration of D1 and D2 receptor agonist have any effect on 6-OHDA induced motor deficits in rats. We assessed locomotor activity (distance travelled in cm) by Optovarimax (Fig. 2A). Our results demonstrate that 6-OHDA lesioned rat showed significant reduction in distance travelled as compared to control rats (Fig. 2A, P < 0.001). Interestingly, D1 receptor agonist SKF-38393 and D2 receptor agonist Bromocriptine treatment in 6-OHDA lesioned rats potentially improved distance travelled as compared to 6-OHDA lesioned rats (Fig. 2A, P < 0.05, P < 0.05). In contrast, this positive effect of D1 or D2 receptor agonists on locomotor activity in 6-OHDA lesioned rats was reversed following cotreatment with D1 antagonist SCH-23390 and D2 antagonist raclopride, suggesting that SCH-23390 and raclopride antagonize the effect of the D1 and D2 receptor agonists, respectively (Fig. 2A). We also found significantly increased locomotor activity in L-DOPA treated 6-OHDA lesioned rat as compared to 6-OHDA lesioned rat (Fig. 2A, P < 0.001).

Next, we performed rotarod test for assessing neuromuscular coordination of 6-OHDA lesioned rats (Fig. 2B). Interestingly, SKF-38393 treatment significantly attenuated 6-OHDA induced latency to fall as compared to 6-OHDA lesioned group (Fig. 2B, P < 0.01). However this improvement in motor coordination was blocked by cotreatment with D1 antagonist SCH-23390 (Fig. 2B). In contrast, we did not find any significant effect of bromocriptine and raclopride treatment on latency to fall in 6-OHDA lesioned rat (Fig. 2B, P > 0.05). Additionally, L-DOPA treatment in 6-OHDA lesioned rats resulted in significant improvement in latency to fall as compared to 6-OHDA lesioned group (Fig. 2B, P < 0.001).

Further, we monitored amphetamine induced ipsilateral rotations to assess the effect of dopamine receptors agonist and antagonist on 6-OHDA mediated unilateral degeneration of presynaptic DAergic neuron terminals (Fig. 2C). 6-OHDA lesioned rats exhibited significantly higher net ipsilateral rotational score as compared to control rats (Fig. 2C, P < 0.001). SKF-38393 and bromocriptine treatment in 6-OHDA lesioned rat significantly decreased amphetamine induced net ipsilateral rotations when compared with 6-OHDA-lesioned group (Fig. 2C, P < 0.001, P < 0.01). Moreover, the effect of SKF-38393 and Bromocriptine on ipsilateral rotations was attenuated by cotreatment with SCH-23390 or raclopride in respective group. Interestingly, L-DOPA treated 6-OHDA lesioned rats also displayed significant reduction in amphetamine induced net ipsilateral rotations when compared with 6-OHDA-lesioned group (Fig. 2C, P < 0.001).

3.3. D1 receptor agonism protects DAergic neurons and restores dopamine levels against 6-OHDA induced neurotoxicity

To investigate the role of dopamine receptor on 6-OHDA induced DAergic neuronal loss in SNpc and axon terminal loss in striatum region, we performed immunostaining of tyrosine hydroxylase (TH), a marker of DAergic neurons (Fig.3A and C). 6-OHDA lesioned rats showed significantly decreased TH^+ cells in SNpc and TH intensity in striatum region as compared to the control group (Fig. 3B, P < 0.001 and D, P < 0.001). SKF-38393 treatment significantly rescued the 6-OHDA induced loss of TH^+ cells in SNpc and TH intensity in striatum as compared to 6-OHDA lesioned group (Fig. 3B, P < 0.05 and D, P < 0.01). However, the effect of SKF-38393 on TH^+ neurons and TH intensity was blocked by cotreatment with SCH-23390 (Fig. 3B and D). In contrast, Bromocriptine and raclopride treatment in 6-OHDA lesioned rats did not show any effect on TH^+ neurons and TH intensity when compared with 6-OHDA lesioned group (Fig. 3B, P > 0.05 and D, P > 0.05). Interestingly, L-DOPA treatment in 6-OHDA lesioned rats also significantly improved the number of TH^+ neurons and the TH intensity (Fig. 3B, P < 0.05 and D, P < 0.001).

Next, we measured the dopamine levels in ipsilateral striatum region using high-performance liquid chromatography (HPLC) coupled with PDA detector (Fig. 4A). SKF-38393 and bromocriptine treatment in 6-OHDA rats significantly restored 6-OHDA induced loss of dopamine content in striatum region (Fig. 4A, P < 0.001, P < 0.01). Interestingly, the effect of D1 and D2 agonists on dopamine levels in 6-OHDA lesioned rats was attenuated following cotreatment with D1 receptor antagonist SCH-23390 and D2 receptor antagonist raclopride respectively (Fig. 4A and B). Additionally, L-DOPA treatment in 6-OHDA lesioned rats similarly increased dopamine levels in striatum region as compared to 6-OHDA lesioned rats (Fig. 4A, P < 0.001).

Next, we investigated the possibility of D1 receptor induced mitochondrial density in DAergic neurons. Therefore, to ascertain our notion, we performed double immunostaining of TH and COX-IV (mitochondrial marker) in SNpc region (Fig. 5A). The number of TH^+/$COX\text{-}IV^+$ cells was significantly reduced in SNpc in 6-OHDA lesioned rats as compared to control rats (Fig. 5B, P < 0.001). Interestingly, D1 receptor agonist SKF-38393 treated 6-OHDA lesioned rats exhibited significantly increased number of $TH^+/COX\text{-}IV^+$ cells in the SNpc as compared to 6-OHDA lesioned rats (Fig. 5B, P < 0.001). In contrast, this effect of SKF-38393 was blocked by cotreatment with D1 antagonist SCH-23390. Bromocriptine and co-treatment with raclopride showed no effect on $TH^+/COX\text{-}IV^+$ cells, when compared with 6-OHDA lesioned group. Similar to D1 agonist effect, L-DOPA treatment also significantly increased the number of $TH^+/COX\text{-}IV^+$ cells in 6-OHDA lesioned rats when compared with 6-OHDA lesioned rats (Fig. 5B, P < 0.001).

3.4. D1 receptor agonist improves mitochondrial membrane potential (MMP, Ψ_M) in 6-OHDA induced rat model of PD-like phenotypes

To assess the relative change in mitochondrial membrane potential in freshly isolated mitochondria, we used mitochondrial lipophilic cationic florescent dye JC-1. SKF- 38393 treatment in 6-OHDA lesioned rats markedly restored MMP in SNpc (Fig. 6B, P < 0.001). In contrast, cotreatment with SCH-23390 in 6-OHDA lesioned rats blocked this effect of SKF-38393 on MMP in SNpc as compared to 6-OHDA lesioned group (Fig. 6B). However bromocriptine treatment and cotreatment with raclopride in 6-OHDA lesioned rat did not show any significant

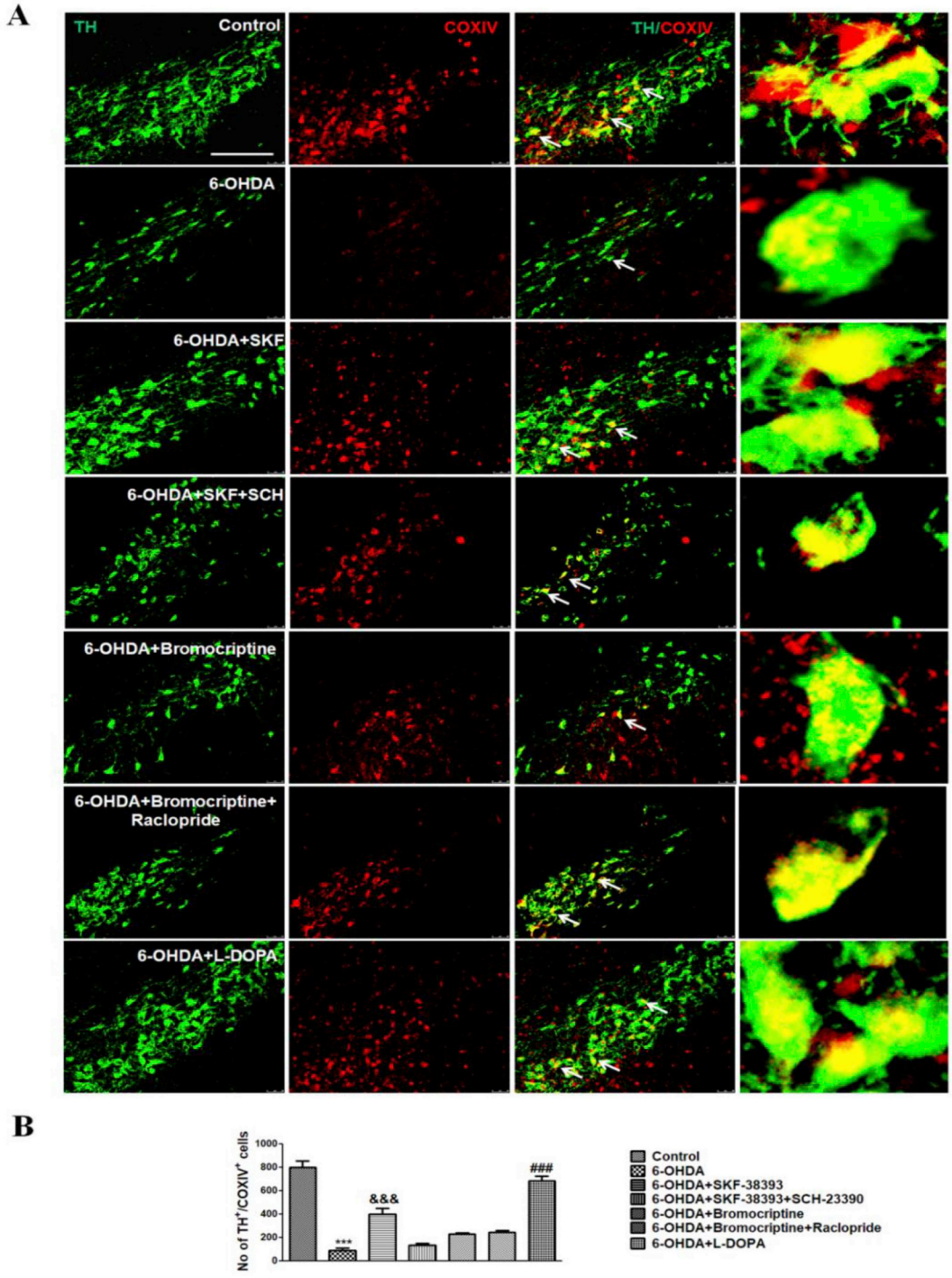

Fig. 5. D1 receptor activation enhance mitochondrial density in dopaminergic neuron in 6-OHDA induced rat model of PD. Representative photomicrographs depict immunostaining of COX-IV (a mitochondrial density marker; red) and TH (a marker of DAergic neurons; blue), in the SNpc on 21 day after 6-OHDA injection. **(B)** Bar graph shows quantification of COX-IV^{+}/TH^{+} cells in the SNpc. Data were analyzed by One-way ANOVA followed by Bonferroni's Multiple Comparison Test ($^{*}P < 0.05$, $^{**}P < 0.01$, $^{***}P < 0.001$, $^{\&}P < 0.05$, $^{\&\&}P < 0.01$, $^{\&\&\&}P < 0.001$, $^{\#}P < 0.05$, $^{\#\#}P < 0.01$, $^{\#\#\#}P < 0.001$) * = Control vs 6-OHDA, & = 6-OHDA vs 6-OHDA + SKF-38393, # = 6-OHDA vs 6-OHDA + L-DOPA.

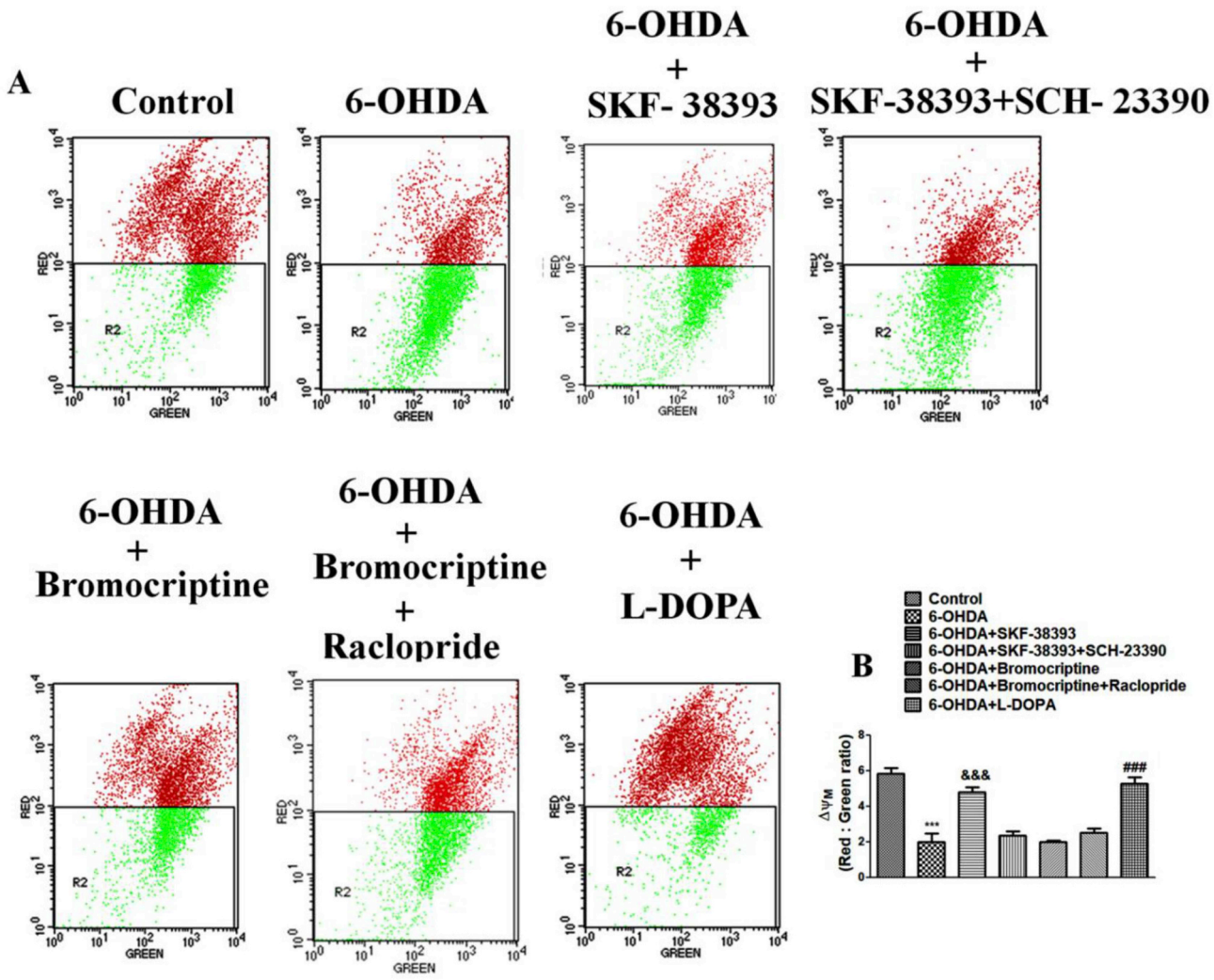

Fig. 6. D1 receptor stimulation increases mitochondrial membrane potential in 6-OHDA induced rat model of PD. Mitochondrial membrane potential ($\Delta\Psi_M$) was measured by FACS analysis using JC-1 dye and red vs green fluorescence ratio was quantified to determine $\Delta\Psi_M$. In panels **A**, representative dot plots from a single analysis are shown. Gated region R2 (green) includes depolarized mitochondria with loss of Ψ_M, whereas red gated region depicts healthy mitochondria with intact Ψ_M.**(B)** Bar graph shows $\Delta\Psi_M$ (red: green ratio) in the SNpc region. Data were analyzed by One-way ANOVA followed by Bonferroni's Multiple Comparison Test ($^{*}P < 0.05$, $^{**}P < 0.01$, $^{***}P < 0.001$, $^{\&}P < 0.05$, $^{\&\&}P < 0.01$, $^{\&\&\&}P < 0.001$, $^{\#}P < 0.05$, $^{\#\#}P < 0.01$, $^{\#\#\#}P < 0.001$) * = Control vs 6-OHDA, & = 6-OHDA vs 6-OHDA + SKF-38393, # = 6-OHDA vs 6-OHDA + L-DOPA.

effect on MMP ($\Delta\Psi_M$) in SNpc as compared to 6-OHDA lesioned group (Fig. 5B, $P > 0.05$). Further, we also found the 6-OHDA induced MMP ($\Delta\Psi_M$) loss was significantly recovered by the treatment of L-DOPA (Fig. 6B, $P < 0.001$).

3.5. D1 receptor agonism restores 6-OHDA induced impairment in mitochondrial function in the SNpc

Mitochondrial homeostasis impairment substantially contributes in pathophysiology of PD and degeneration of DAergic neurons in the nigrostriatal pathway. Therefore, to further determine the functional involvement of dopamine receptors in mitochondrial functionality, we measured the citrate synthase activity, ATP level, mitochondrial reactive oxygen species (ROS) levels, and total ROS in SNpc region (Fig. 7). We found that citrate synthase activity (Fig. 7A, $P < 0.001$) and ATP levels (Fig. 7A, $P < 0.01$) were reducedwhereas mitochondrial (Fig. 7D, $P < 0.01$) and total ROS levels (Fig. 7E, $P < 0.001$) were increased significantly in the SNpc in 6-OHDA lesioned rats as compared to control group. Fig. 7. Interestingly, SKF-38393 treated 6-OHDA lesioned rats showed significantly increased citrate synthase activity, ATP level and reduced mitochondrial and total ROS in SNpc as compared to 6-OHDA lesioned group (Fig. 7A, $P < 0.05$, B, $P < 0.05$, D, $P < 0.05$, E, $P < 0.001$). In contrast, cotreatment with D1 receptor antagonist SCH-23390 in 6-OHDA + SKF-38393 treated rats abolished the effect of D1 agonist SKF-38393 on citrate synthase activity, ATP level, mitochondrial ROS and total ROS formation in SNpc region (Fig. 7A-E). However, ATP level, citrate synthase activity, mitochondrial ROS and total ROS formation were not significantly altered in 6-OHDA lesioned rats following treatment with Bromocriptine or co-treatment with D2 antagonist raclopride, when compared with 6-OHDA lesioned rats (Fig. 7A-E, $P > 0.05$). On the other hand, L-DOPA treatment in 6-OHDA lesioned rats showed subtle increase in ATP level and citrate synthase activity and reduction in mitochondrial ROS and total ROS formation in the SNpc as compared to 6-OHDA lesioned group (Fig. 7A, $P < 0.001$, B, $P < 0.01$, D, $P < 0.001$, E, $P < 0.001$).

3.6. D1 receptor stimulation promotes mitochondrial biogenesis in 6-OHDA induced rat model of PD-like phenotypes

Our previous results suggest enhanced mitochondrial functions and mitochondrial density in DAergic neurons that raises the possibility of improved mitochondrial biogenesis in the SNpc. Therefore, we

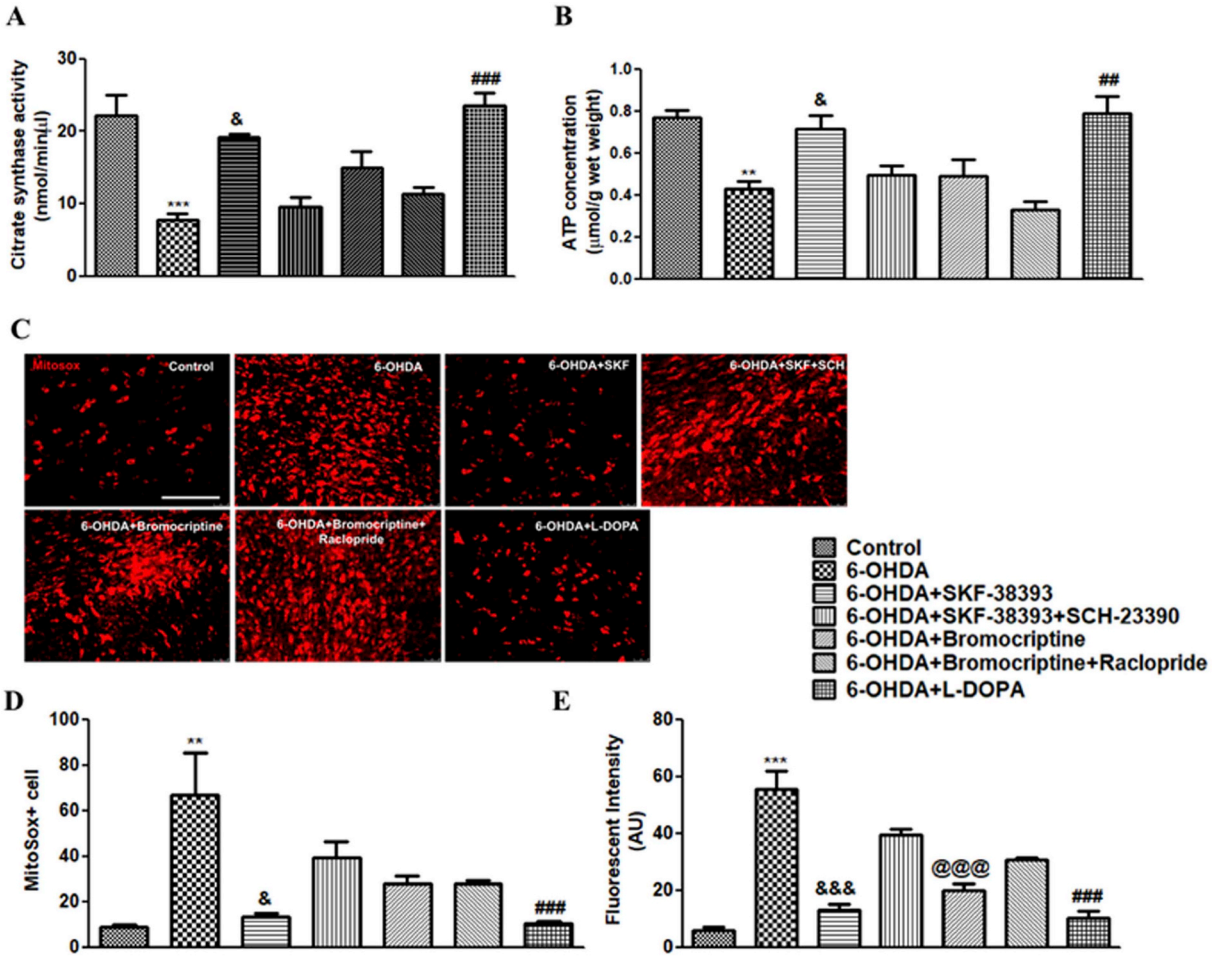

Fig. 7. D1 receptor activation attenuates impairment in mitochondrial functionality in rat model of PD. **(A)** Bar graph shows citrate synthase activity in SNpc. **(B)** Bar graph shows concentration of ATP in SNpc region. **(C)** Representative photomicrographs depict MitoSOx staining in the SNpc region **(D)** Bar graph shows mitochondrial ROS generation in SNpc region, as measured by MitoSox dye **(E)** Bar graph shows the ROS generation in SNpc region, as measured by DCFDA dye. Data were analyzed by One-way ANOVA followed by Bonferroni's Multiple Comparison Test (*$P < 0.05$, **$P < 0.01$, ***$P < 0.001$, $^{\&}P < 0.05$, $^{\&\&}P < 0.01$,$^{\&\&\&}P < 0.001$ $^{@}P < 0.05$, $^{@@}P < 0.01$,$^{@@@}P < 0.001$, $^{\#}P < 0.05$, $^{\#\#}P < 0.01$, $^{\#\#\#}P < 0.001$) * = Control vs 6-OHDA, & = 6-OHDA vs 6-OHDA + SKF-38393, @ = 6-OHDA vs 6-OHDA + Bromocriptine, # = 6-OHDA vs 6-OHDA + L-DOPA.

examined the levels of proteins involved in mitochondrial fusion and fission process in SNpc (Fig. 8A). DRP-1 (Fig. 8B, $P < 0.001$) and Fis-1 (Fig. 8C, $P < 0.001$) levels were significantly up regulated and Mfn-2 (Fig. 8D, $P < 0.01$), OPA-1 (Fig. 8E, $P < 0.001$) and TFAM (Fig. 8F, $P < 0.001$) levels were significantly down-regulated in SNpc in 6-OHDA lesioned rats as compared to control rats. In contrast, SKF- 38393 treated 6-OHDA lesioned rat showed significantly decreased DRP-1 (Fig. 8B, $P < 0.01$) and Fis-1 (Fig. 8C, $P < 0.001$) while significantly increased Mfn-2 (Fig. 8D,$P < 0.05$), OPA-1 (Fig. 8E, $P < 0.01$) and TFAM (Fig. 8F, $P < 0.01$) levels in the SNpc as compared to 6-OHDA lesioned group. However, cotreatment with D1 receptor antagonist SCH-23390 in 6-OHDA + SKF-39393 treated rats potentially reduced the effect of D1 agonist SKF-38393 on Fis-1, DRP-1, Mfn-2, OPA-1 and TFAM protein levels. In contrast, Bromocriptine and raclopride did not show any effect in fusion and fission related protein expression. Interestingly, L-DOPA treated 6-OHDA lesioned rats also displayed significantly decreased expression of DRP-1 (Fig. 8B, $P < 0.001$) and Fis-1 (Fig. 8C, $P < 0.001$) and significantly increased level of Mfn-2 (Fig. 8D, $P < 0.05$), OPA-1 (Fig. 8E, $P < 0.05$) and TFAM (Fig. 8F, $P < 0.001$) in SNpc as compared to 6-OHDA lesioned rat.

3.7. D1 receptor agonism alleviates DAergic neurogenesis in 6-OHDA induced rat model of PD-like phenotypes

We investigated the effect of dopamine receptors on neuronal differentiation. We performed double-immunostaining of BrdU (cell proliferation marker) and DCX (immature neuron/neuroblasts marker) in SNpc region. We found that D1 receptor agonist SKF-38393 treatment significantly enhanced the number of $BrdU^+/DCX^+$ cells (Fig. S1B, $P < 0.01$) as compared to saline treated 6-OHDA lesioned rats. In contrast, cotreatment with D1 receptor antagonist SCH-23390 in 6-OHDA + SKF-39393 treated rats abolished the effect of D1 receptor agonist SKF-38393 on $BrdU^+/DCX^+$ cells (Fig. S1B). However, D2 receptor agonist bromocriptine and cotreatment with D2 receptor antagonist raclopride did not alter the number of $BrdU^+/DCX^+$ cells (Fig. S1B, $P > 0.05$) in SNpc in 6-OHDA lesioned rats. Similarly, L-DOPA treated 6-OHDA lesioned rats showed significantly increased number of $BrdU^+/DCX^+$ cells (Fig. S1B) as compared to 6-OHDA lesioned rats.

Next, we were interested to examine the role of dopamine receptor on DAergic newborn neuron formation. We performed double-immunostaining of TH (DAergic neuronal marker) and BrdU (cell

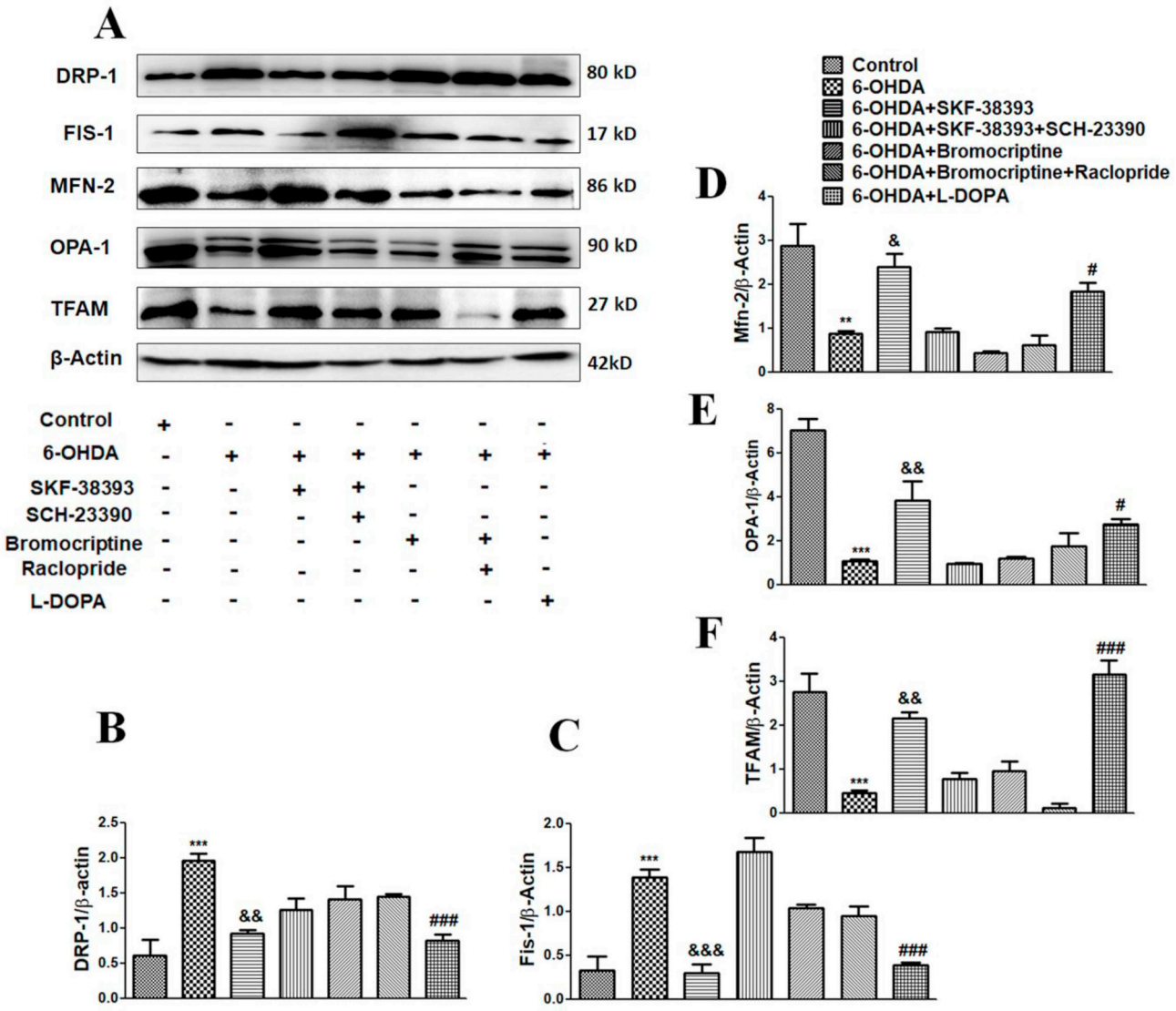

Fig. 8. D1 receptor activation improves mitochondrial biogenesis in the SNpc in 6-OHDA induced rat model of PD-like phenotypes. **(A)** Representative Immunoblots show expression of DRP-1, Fis-1, Mfn-2, OPA-1 and TFAM. Bar graphs show the quantification of the relative protein density of **(B)** DRP, **(C)** Fis-1, **(D)** Mfn-2**(E)** OPA-1, and **(F)** TFAM. The protein density was normalized with density of β-actin. Data were analyzed by One-way ANOVA followed by Bonferroni's Multiple Comparison Test (*$P < 0.05$, **$P < 0.01$, ***$P < 0.001$, $^{\&}P < 0.05$, $^{\&\&}P < 0.01$, $^{\&\&\&}P < 0.001$, $^{\#}P < 0.05$, $^{\#\#}P < 0.01$, $^{\#\#\#}P < 0.001$) * = Control vs 6-OHDA, & = 6-OHDA vs 6-OHDA + SKF-38393, # = 6-OHDA vs 6-OHDA + L-DOPA.

proliferation marker) in the SNpc (Fig. 9A). Interestingly, D1 receptor agonist SKF-38393 treatment significantly restored 6-OHDA induced loss in the $TH^+/BrdU^+$ cells as compared to 6-OHDA lesioned rat (Fig. 9B, $P < 0.001$). In contrast, cotreatment with D1 receptor antagonist SCH-23390 in 6-OHDA + SKF-39393 treated rats reversed the effect of D1 receptor agonist SKF-38393 on $TH^+/BrdU^+$ cells (Fig. 9B). However, D2 receptor agonist bromocriptine and cotreatment with D2 receptor antagonist raclopride the number of $TH^+/BrdU^+$ cells did not alter in SNpc in 6-OHDA lesioned rats (Fig. 9B, $P > 0.05$). Additionally, L-DOPA treated 6-OHDA lesioned rats showed significantly increased number of $TH^+/BrdU^+$ cells in the SNpc as compared to 6-OHDA lesioned rats (Fig. 9B, $P < 0.001$).

3.8. D1 receptor agonism promotes Wnt/β-catenin signalling in the SNpc in rat model of PD-like phenotypes

We further investigated the mechanistic pathway by which dopamine receptor regulate behavioural function, mitochondrial biogenesis, mitochondrial dynamics and DAergic neurogenesis. Wnt/β-catenin signalling is critically involved in the development and survival of DAergic neurons (Jho et al., 2002). Further, we examined the protein levels of Wnt/β-catenin signalling mediators by immunoblotting (Fig. 10A). Protein levels of p-Tyr216 GSK-3β (Fig. 10B, $P < 0.001$), Axin-2 (Fig. 10C, $P < 0.01$), APC (Fig. 10D, $P < 0.001$) and p-β-catenin (Fig. 10E, $P < 0.001$) were increased in cytosolic fraction and the level of non-phosphorylated β-catenin (Fig. 10F, $P < 0.001$ and G, $P < 0.001$) was reduced significantly in cytosolic and nuclear fraction of SNpc in 6-OHDA lesioned rat as compared to control group. D1 receptor agonist SKF-38393 treatment in 6-OHDA lesioned rat significantly decreased p-Tyr216 GSK-3β (Fig. 10B, $P < 0.001$), Axin-2 (Fig. 10C, $P < 0.001$), APC (Fig. 10D, $P < 0.01$) and p-β-catenin (Fig. 10E, $P < 0.001$) level in cytosolic fraction and enhanced non-phosphorylated β-catenin levels (Fig. 10F, $P < 0.001$ and G, $P < 0.01$) in cytosolic and nuclear fractions in SNpc as compared to 6-OHDA lesioned rats. In contrast, cotreatment with D1 receptor antagonist SCH-23390 in 6-OHDA + SKF-39393 treated rats attenuated

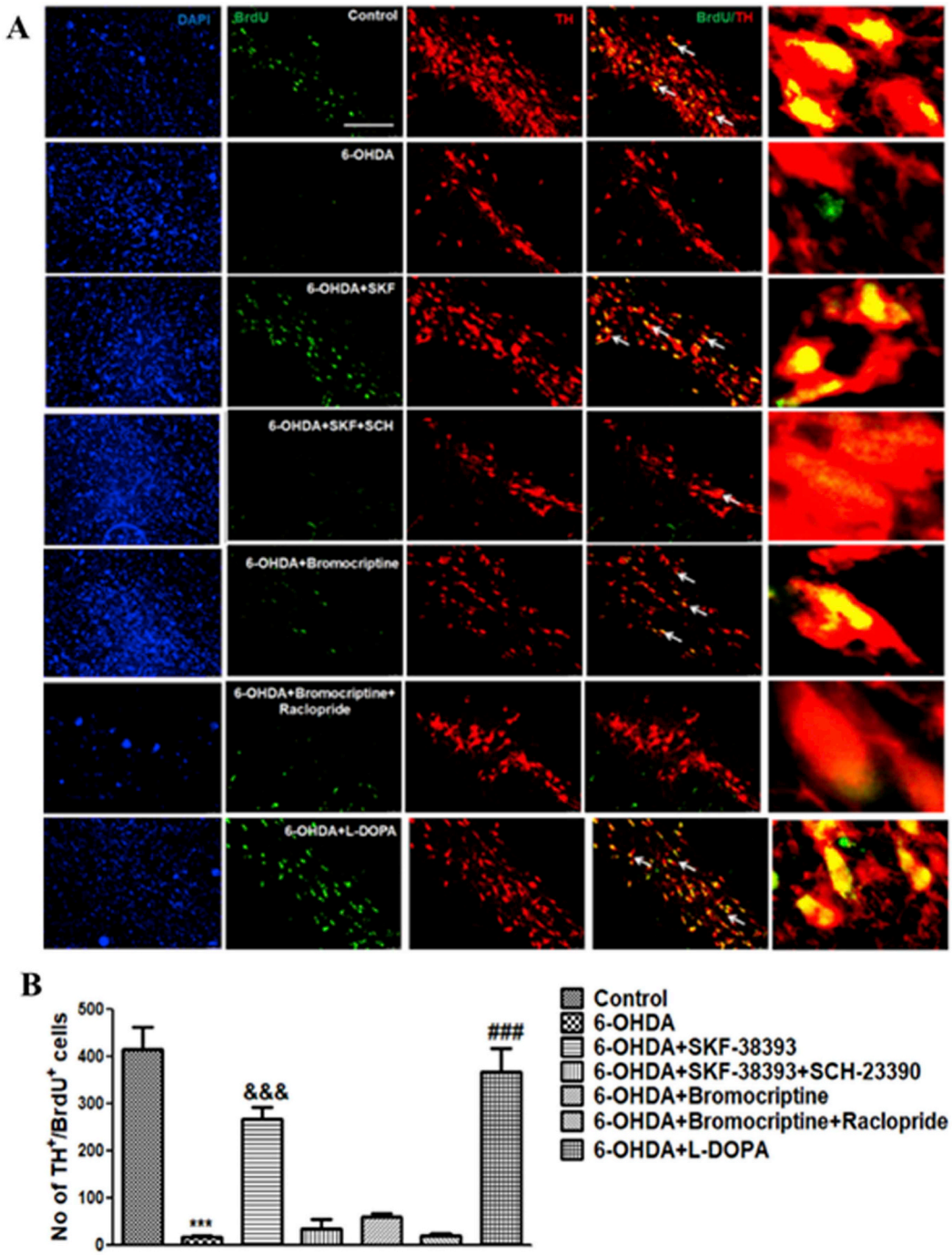

Fig. 9. D1 receptor Activation attenuates 6-OHDA-induced depletion of newborn DAergic neurons in parkinsonian rats. **(A)** Representative photomicrographs shows immunostaining of BrdU (a cell proliferation marker; green) and TH (a marker of DAergic neurons; red), in SNpc on 21 day after 6-OHDA injection **(B)** Bar graph shows quantification of $TH^+/BrdU^+$ cells in the SNpc. Data were analyzed by One-way ANOVA followed by Bonferroni's Multiple Comparison Test (*P < 0.05, **P < 0.01, ***P < 0.001, $^{\&}$P < 0.05, $^{\&\&}$P < 0.01,$^{\&\&\&}$P < 0.001,#P < 0.05, ##P < 0.01, ###P < 0.001) * = Control vs 6-OHDA, & = 6-OHDA vs 6-OHDA + SKF-38393, # = 6-OHDA vs 6-OHDA + L-DOPA.

the effect of D1 agonist on Wnt signalling related proteins. Additionally, we did not find any significant effect of D2 receptor agonist bromocriptine treatment or cotreatment with D2 receptor antagonist raclopride on Wnt pathway related proteins in 6-OHDA lesioned rats. L-DOPA treated 6-OHDA lesioned rats showed significantly decreased levels of p-Tyr216-GSK-3β (Fig. 10B, P < 0.01), Axin-2 (Fig. 10C, P < 0.001), APC (Fig. 10D, P < 0.01) and p-β-catenin (Fig. 10E, P < 0.001) in cytosolic fraction and increased levels of non-phosphorylated β-catenin level (Fig. 10F, P < 0.001 and G, P < 0.01) in cytosolic and nuclear fraction of SNpc when compared with 6-OHDA lesioned rats.

3.9. Axin-2 knockdown in D1 antagonist SCH-23390 treated PD rats improves mitochondrial functions, DAergic neurogenesis and behavioural functions

Further, to clarify the involvement of Wnt/β-catenin signalling in D1 receptor mediated neuroprotection in rat model of PD-like

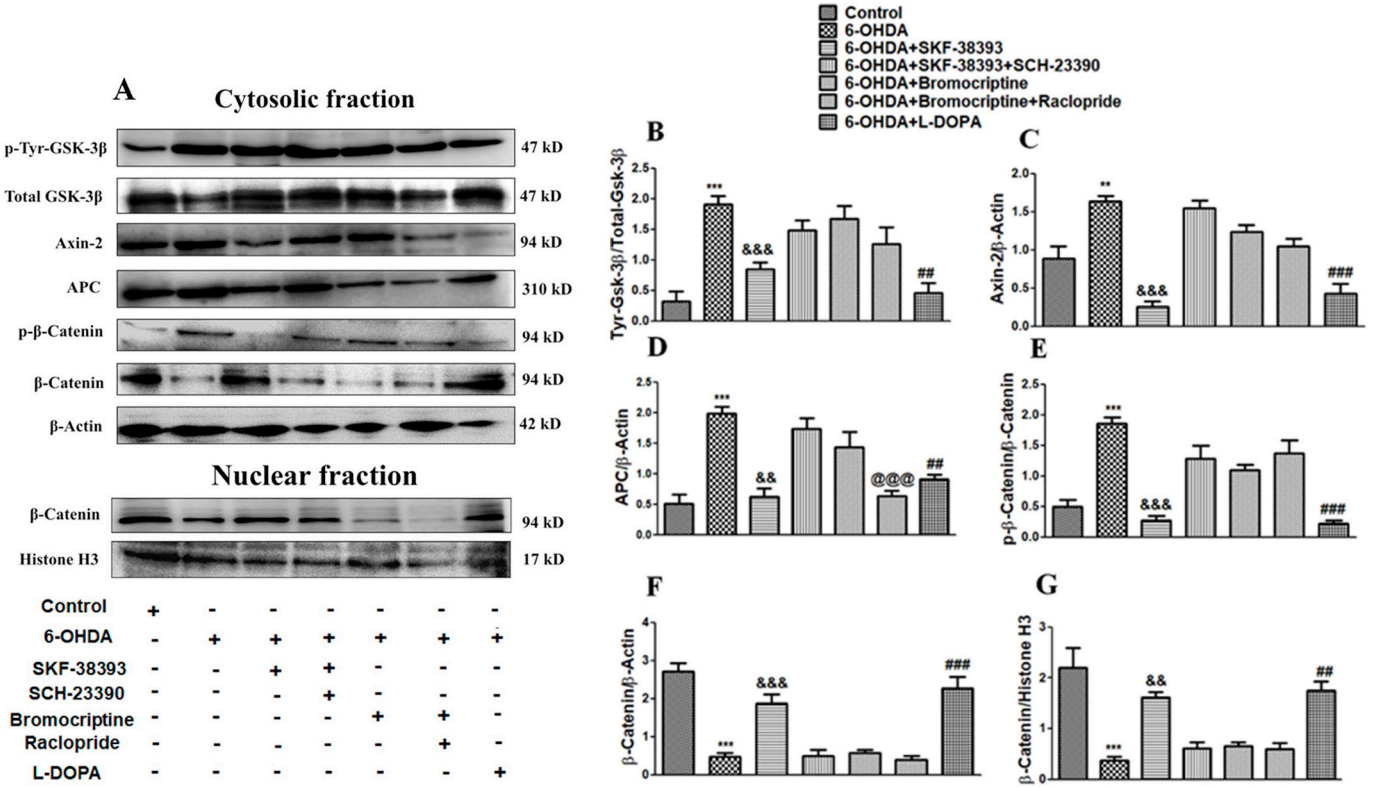

Fig. 10. D1 receptor activates Wnt/β-catenin signalling in the SNpc of parkinsonian rats. **(A)** Representative Immunoblots show expression of p-Tyr216 GSK-3β, non-phosphorylated (total) GSK-3β, Axin2, APC, p-β-catenin and β-catenin in cytosolic fraction and β-catenin in nuclear fraction. Bar graphs show quantification of the relative protein density of **(B)** p-Tyr216 GSK-3β **(C)** Axin-2, **(D)** APC **(E)** p-β-catenin and **(F)** β-catenin in cytosolic fraction.**(G)** Bar graph shows quantification of the relative protein density of β-catenin in nuclear fraction. The protein density of p-Tyr216-GSK-3β was normalized with total GSK-3β protein density and the density of other proteins was normalized with β-actin in cytosolic fraction. The protein density of β-catenin was normalized with Histone H3 protein density in nuclear fraction Data were analyzed by One-way ANOVA followed by Bonferroni's Multiple Comparison Test (*P < 0.05, **P < 0.01, ***P < 0.001, &P < 0.05, &&P < 0.01,&& &P < 0.001 @P < 0.05, @@P < 0.01,@@@P < 0.001, #P < 0.05, ##P < 0.01, ###P < 0.001) * = Control vs 6-OHDA, & = 6-OHDA vs 6-OHDA + SKF-38393, @ = 6-OHDA vs 6-OHDA + Bromocriptine, # = 6-OHDA vs 6-OHDA + L-DOPA.

phenotypes, we stereotaxically injected Axin-2 shRNA into SNpc. Axin-2 is a member of β-catenin degradation complex, hence acts as a negative regulator of Wnt/β-catenin signalling (Jho et al., 2002). Interestingly, cotreatment of Axin-2 shRNA with D1 receptor antagonist SCH-23390 in 6-OHDA rats decreased p-Tyr216-GSK-3β (Fig. 11 B, $P < 0.001$), Axin-2 (Fig. 11C, $P < 0.001$), APC (Fig. 11D, $P < 0.001$) and p-β-catenin (Fig. 11E, $P < 0.001$) levels and increased non-phosphorylated β-catenin levels (Fig. 11F, $P < 0.001$ and G, $P < 0.001$) significantly in cytosolic as well as nuclear fraction, when compared with 6-OHDA + SKF-38393 + SCH-23390 treated 6-OHDA lesioned rats.

We also found enhanced distance travelled in open-field activity test and reduced latency and net ipsilateral rotations in Axin-2 knockdown D1 antagonist SCH-23390 treated 6-OHDA lesioned rats as compared to 6-OHDA + SKF-38393 + SCH-23390 treated rats (Fig. 12A, $P < 0.05$, B, $P < 0.001$ and C, $P < 0.001$). Interestingly, the number of TH^+/$BrdU^+$ cells were significantly increased in the SNpc in Axin-2 knockdown D1 antagonist SCH-23390 treated 6-OHDA lesioned rats as compared to 6-OHDA + SKF-38393 + SCH-23390 treated rats (Fig. 13B, $P < 0.001$).

Further, to determine the role of Wnt/β-catenin pathway in mitochondrial functionality, we analyzed citrate synthase activity and ATP levels in D1 antagonist SCH-23390 treated PD rats. The citrate synthase activity and ATP level was significantly increased in Axin-2 knockdown D1 antagonist SCH-23390 treated 6-OHDA lesioned rat in SNpc as compared to 6-OHDA + SKF-38393 + SCH-23390 treated rats (Fig. 14A, $P < 0.05$ and B, $P < 0.001$).

4. Discussion

In the present study, we demonstrate that single unilateral administration of 6-OHDA reduced D1 receptor level in the SNpc. 6-OHDA induced motor behaviour impairment, mitochondrial dysfunction, degeneration of nigral DAergic neurons and reduced formation of newborn DAergic neurons associated with down-regulation of D1 receptor mediated Wnt/β-catenin signaling in the SNpc.

Mounting evidences suggest a significant progress in understanding the functional and structural basis of dopamine receptors during behavioural response, long-term plasticity and cognitive functions by multilevel interaction with other messengers, such as glutamate, serotonin and GABA using pharmacological, genetic and molecular tools (Fiorentini et al., 2006; Singh et al., 2018b). Recent studies have focused on uncovering the complexity, redundancy, intricacy and cellular and molecular mechanism involved in dopamine receptor mediated effects (Hedlund et al., 2016; Maurice et al., 2004; Tozzi et al., 2018; Winner et al., 2009). We found that single intra-MFB administration of 6-OHDA decreased D1 receptor level, DAergic axonal density in the striatum and cell bodies the SNpc leading to reduction in dopamine content in the midbrain of adult rats brain. These observations are further supported by previous studies (Mishra et al., 2019; Singh et al., 2018b). D1 receptor agonist treatment restored D1 level, axonal density, number of DAergic neurons and dopamine content in midbrain of 6-OHDA lesioned rats. Additionally, D1 receptor agonism attenuated 6-OHDA induced motor impairment and amphetamine induced net ipsilateral rotations, indicating a positive effect of D1 receptor stimulation

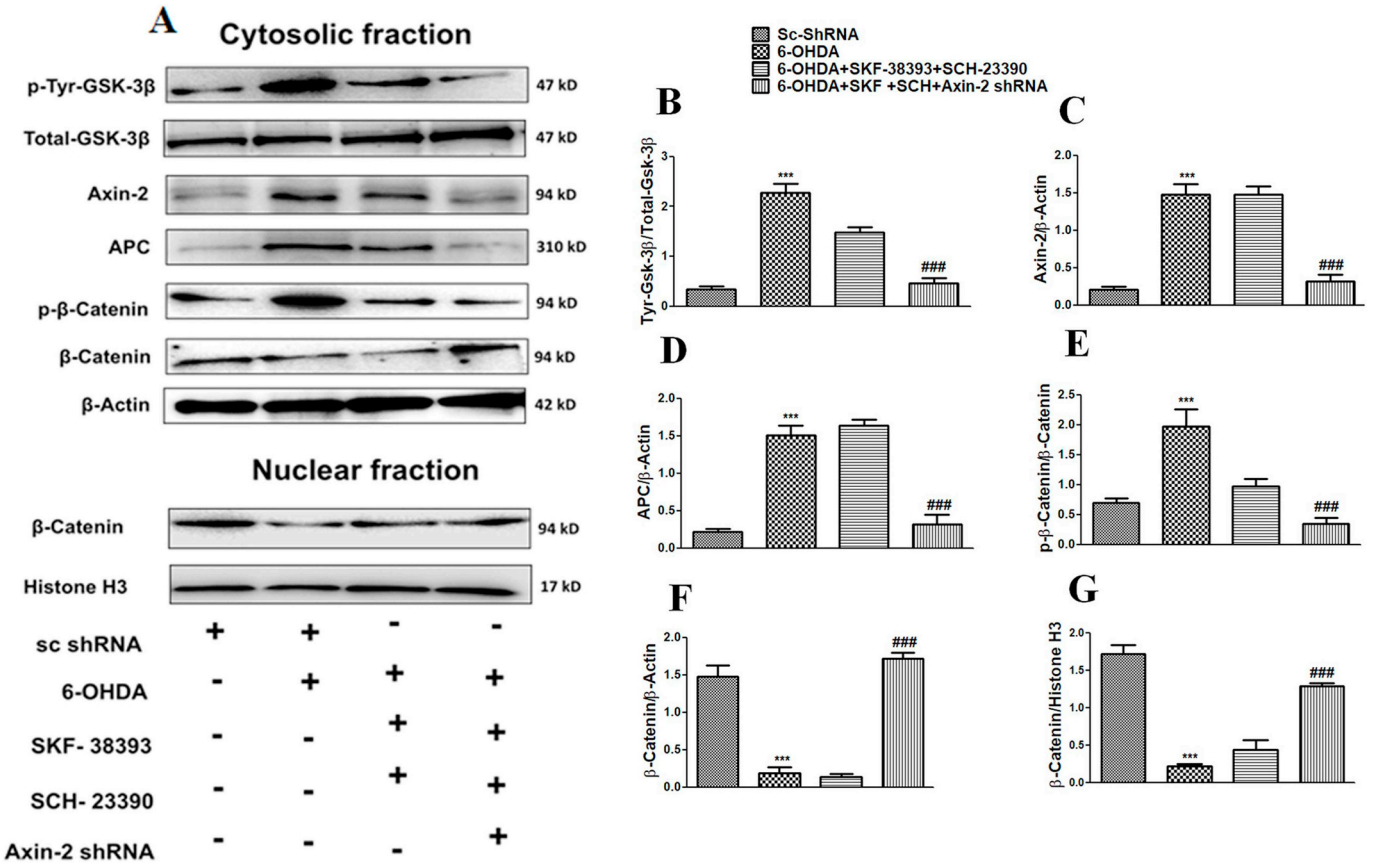

Fig. 11. Axin-2- shRNA activates Wnt/β-catenin signalling in D1 receptor antagonist SCH-23390 treated 6-OHDA lesioned rat in SNpc. **(A)** Representative Immunoblots show expression of p-Tyr216 GSK-3β, non-phosphorylated (total) GSK-3β, Axin2, APC, p-β-catenin and β-catenin in cytosolic fraction and β-catenin in nuclear fraction. Bar graphs show quantification of relative protein density of **(B)** p-Tyr216 GSK-3β **(C)** Axin-2, **(D)** APC **(E)** p-β-catenin and **(F)** β-catenin in cytosolic fraction. **(G)** Bar graph shows the quantification of relative protein density of β-catenin in nuclear fraction. The protein density of p-Tyr216-GSK-3β was normalized with total GSK-3β protein density and the density of other proteins was normalized with β-actin in cytosolic fraction. Phosphorylated-β-catenin level was normalized with nonphosphorylated-β-catenin in cytosolic fraction. The protein density of β-catenin was normalized with Histone H3 protein density in nuclear fraction Data were analyzed by One-way ANOVA followed by Bonferroni's Multiple Comparison Test (*P < 0.05, **P < 0.01, ***P < 0.001, $^{\#}$P < 0.05, $^{\#\#}$P < 0.01, $^{\#\#\#}$P < 0.001) * = scshRNAvs 6-OHDA + scshRNA, # = 6-OHDA + scshRNAvs 6-OHDA + Axin-2 shRNA.

on dopamine system activation and associated behavioural function in PD rats. Interestingly, the effects of D1 agonist on behavioural activity in 6-OHDA lesioned rats were attenuated following the treatment with D1 antagonist SCH-23390. However, D2 agonist Bromocriptine and antagonist raclopride had no significant effect on motor incoordination in PD rats, suggesting a preferential effect of D1 receptor stimulation on locomotor activity in PD rats. Interestingly, pharmacological treatment with D1 antagonist SCH-23390 induced impairment in motor co-ordination in control rats, which were reversed by the administration of D1 agonist SKF-82958 (Avila-Luna et al., 2018). The preferential role of D1 stimulation on motor related functions as observed in our study is further supported by the fact that SKF-80723 and SKF-83959 (D1R agonist) increased locomotor activity and also reversed motor disability in MPTP (1-methyl-4-phenyl-1, 2, 3, 6-tetrahydropyridine) treated marmosets (Gnanalingham et al., 1995). Dopamine D1/D2 receptor agonist lisuride (0.001–1 μM) treatment enhances the survival of DAergic neurons in primary culture and protected against L-DOPA and 1-methyl-4-phenylpyridinium ion (MPP^+) induced cytotoxicity (Gille et al., 2002). Similarly, dopamine receptor agonists like pergolide and pramipexole also have been reported to protect DAergic neurons against ageing and MPTP induced loss of midbrain DAergic neurons (Felten et al., 1992; Joyce et al., 2004). Our results demonstrate that D1 receptor agonist SKF-23390 or L-DOPA protects DAergic neurons in SNpc and reduces axonal terminal loss in striatum region which lead to improved dopamine level and behavioural functions in 6-OHDA lesioned rats. Additionally, D2 receptor agonist or antagonist raclopride had no significant neuroprotective effect on DAergic neuronal population against 6-OHDA induced neurotoxicity in adult rats. Our results are further supported by the study showing that DAergic graft in striatum and substantia nigra enhance TH^+ DAergic neuronal population leading to reduced ipsilateral rotations induced by D1 receptor agonist SKF-38393, but not by D2 agonist LY-171555 in 6-OHDA lesioned rats (Robertson et al., 1991).

Dysfunction of mitochondrial dynamics and mitochondrial fission/fusion has been linked to pathogenesis of neurodegenerative disease including PD. 6-OHDA induces ROS production, inhibits complex 1 activity and reduces the ATP production which collectively causes DA depletion in midbrain (Brouillet et al., 1995; Kupsch et al., 2014; Li et al., 2011; Schapira et al., 1989). Several studies have shown that increased production of oxidative products are associated with nigral DAergic neuronal damage in rodent models of PD and post-mortem brain tissues of patients with PD (Alam et al., 1997; Dexter et al., 1994; Floor and Wetzel, 1998). Interestingly, intra-VTA diazepam infusion facilitate social competition and enhances mitochondrial respiration, dopamine levels and activity of dopamine D1-but not D2-containing cells in the nucleus accumbens (NAc). In support of these findings, our results show that D1 receptor agonism improves mitochondrial functions and number of TH^+ and $COX\text{-}IV^+$ cells in SNpc, which were blocked by D1 receptor antagonist SCH-23390 treatment. Consistent with previous studies, our data also suggest that D1 receptor activation

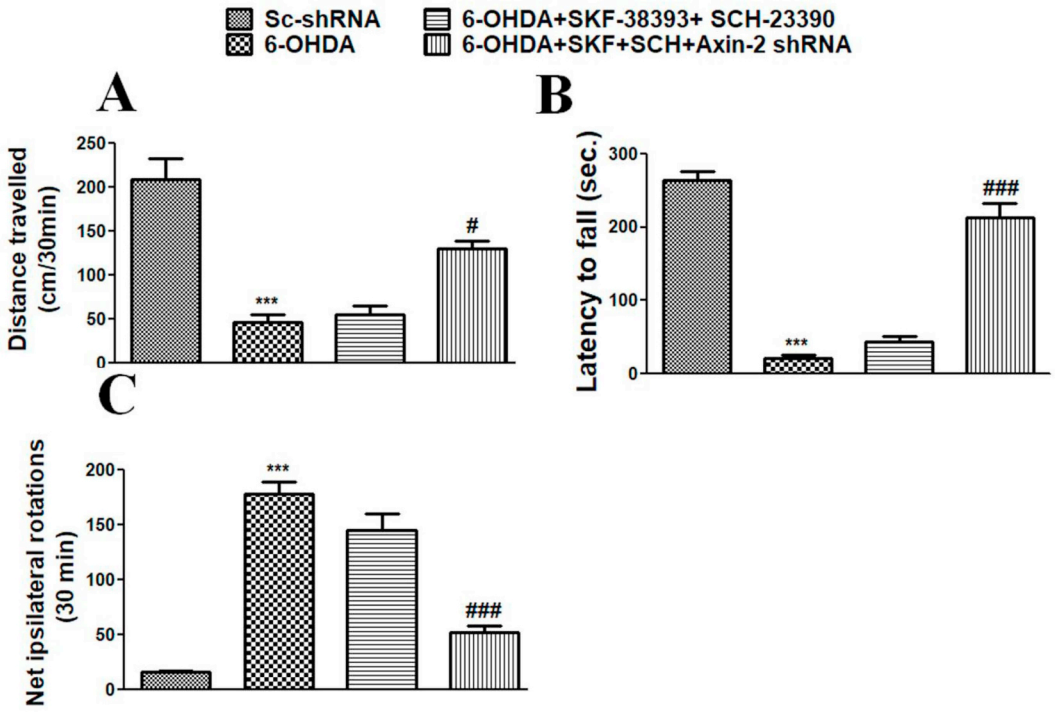

Fig. 12. Wnt/β-Catenin signalling activation enhances behavioural activity in D1 antagonist SCH-23390 treated 6-OHDA lesioned rat (A) Bar graph show the locomotor activity was represented as distance travelled over a 30-min period. **(B)** Bar graph shows the performance on rotarod was evaluated as latency to fall from the rod for a period of 300 s. **(C)** Bar graph shows Amphetamine (5 mg/kg, i. p.)-induced net ipsilateral rotations were observed over a period of 30 min. Data are expressed as mean ± SEM of n = 8 rats/group. Data were analyzed by One-way ANOVA followed by Bonferroni's Multiple Comparison Test (*P < 0.05, **P < 0.01, ***P < 0.001, $^{\#}$P < 0.05, $^{\#\#}$P < 0.01, $^{\#\#\#}$P < 0.001) * = scshRNAvs 6-OHDA + scshRNA, # = 6-OHDA + scshRNAvs 6-OHDA + Axin-2 shRNA.

mediated improved mitochondrial functionality in DAergic neurons may result in increased survival of DAergic neurons in PD rats. Impaired mitochondrial biogenesis have long been hypothesized to play a pathogenic role in neurodegeneration including PD pathogenesis (Scholpa et al., 2018; Singh et al., 2018a; Thomas et al., 2012; Uittenbogaard and Chiaramello, 2014). In particular, pharmacologically increased mitochondrial biogenesis promotes DAergic neuron survival and improves behavioural function in rodents model of PD (Singh et al., 2018a). TFAM is a nuclear encoded protein synthesized in cytosol and transported into mitochondria, where it binds to mitochondrial RNA polymerase to enables transcription initiation (Morozov et al., 2014; Ramachandran et al., 2017). In particular, high level of mtDNA deletions in the SNpc and striatum are observed in post-mortem brain tissue of patients with PD (Bender et al., 2006; Ikebe et al., 1990). Reduction in mtDNA copy number/genome content has been reported in peripheral blood and nigral DAergic neurons of individuals affected with PD (Dolle et al., 2016; Pyle et al., 2016). In contrast, genetic ablation of TFAM in DAergic neurons of mice significantly decreased the mitochondrial DNA content and impaired behavioural activity (Ekstrand et al., 2007). In agreement with these studies, we showed that mitochondrial biogenesis and TFAM levels are reduced following 6-OHDA injection. Additionally, improved mitochondrial biogenesis and mitochondrial functions in the SNpc could be associated with enhanced number of mitochondria in DAergic neurons ($COX\text{-}IV^{+}/TH^{+}$) which lead to increased number of newborn DAergic neurons in SNpc of D1 agonist treated 6-OHDA lesioned rats. However, D1 agonism mediated effects on mitochondrial functions and DAergic neurons were blocked by cotreatment with D1 antagonist. Interestingly, D2 receptor agonism or antagonism did not show any modulatory effects on mitochondrial functions and formation of newborn DAergic neurons, further suggesting a preferential effect of D1 receptor mediated signalling in rat model of PD-like phenotypes. Our data is further supported by the fact that intra-VTA infusion of diazepam increased ATP levels, mitochondrial respiration, DAergic positive cells in nucleus accumbens and social dominance in rats via D1 receptor activation, but these effects were not modulated by D2 receptor agonist (van der Kooij et al., 2018). Additionally, stimulation with either dopamine or D2 receptor agonist directly inhibits mitochondrial motility, whereas pharmacological activation of D1 receptor promotes mitochondrial trafficking in hippocampal neurons (Chen et al., 2008), suggesting energy distribution in the neurons is differentially regulated by D1 and D2 receptors.

However, DAergic modulation in forebrain precursor proliferation is not only restricted in rodents but has also been identified in monkeys (Freundlieb et al., 2006) and humans (Hoglinger et al., 2004). We and others have shown that 6-OHDA induced neurotoxicity reduced proliferation and differentiation capacity of neural progenitors cells (NPCs) in the midbrain region that lead to decreased neurogenic potential in SNpc and striatum region (Winner et al., 2009). Dopamine receptor agonism/antagonism has been reported to modulate different aspects of neurogenesis process, for example, chronic oral administration of dopamine receptor D2/D3 agonist Pramipexole (PPX) promotes DAergic neurogenesis in the SVZ and olfactory bulb as well as improves motor functions in 6-OHDA lesioned rats (Winner et al., 2009). D2/D3 receptor stimulation by PPX, but not Ropinirole enhances NSC proliferation and differentiation into newborn neurons in the hippocampus and striatum of adult mice, suggesting that the effects could also depend on the affinity and regional distribution of NSC (Salvi et al., 2016). In line with this evidence, we observed that D1 receptor agonist administration, but not D2 receptor agonist Bromocriptine, enhances DAergic neurogenesis in 6-OHDA lesioned rats. Interestingly, the effect of D1 agonism on formation of newborn DAergic neurons was blocked by cotreatment of D1 antagonist, suggesting a positive effect of D1 receptor signalling on adult DAergic neurogenesis. D1 and D2 receptors

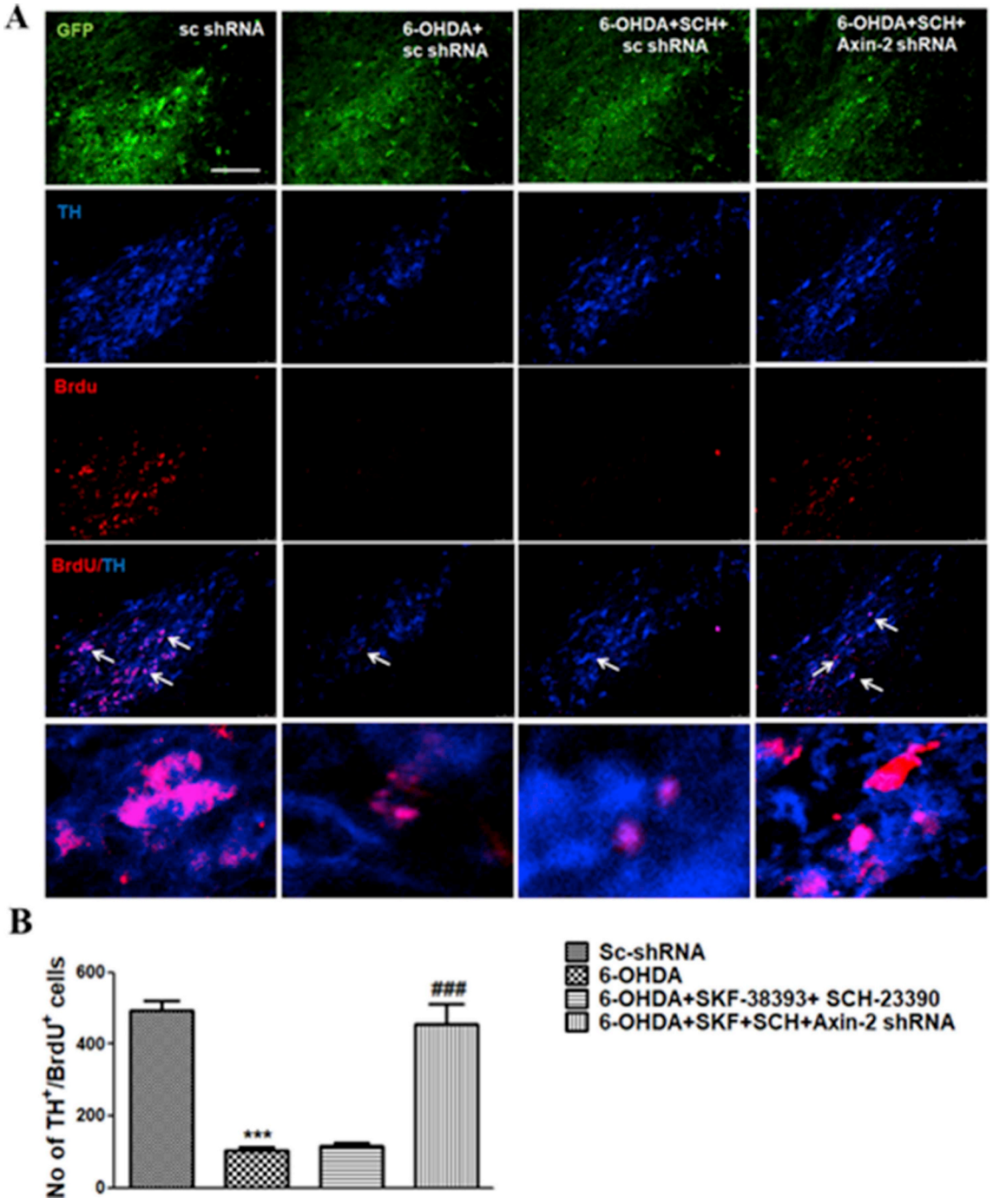

Fig. 13. Wnt/β-Catenin signalling activation restores D1 antagonist SCH-23390 induced reduction in new dopaminergic neurons in SNpc region. **(A).** Represntative photomicrograph show the immunostaining of tyrosine hydroxylase (TH) in blue and bromodeoxyuridine (BrdU) in red colour. **(B).** Bar graph show the number of TH and BrdU double immunolabelled cells in the SNpc.

exert opposing actions and often have different physiological effects. D1 stimulation/activation activates adenylyl cyclase-protein kinase A (AC-PKA) pathway that results in increased intracellular concentration of cyclic adenosine monophosphate (cAMP), a secondary messenger. On the other hand, D2-like receptor stimulation directly reduces the cAMP concentration by inhibiting AC-PKA proteins (Kebabian and Greengard, 1971; Neve et al., 2004; Undieh, 2010). Interestingly, cAMP dependent PKA increased intracellular and nuclear β-catenin levels by inhibiting its proteasomal degradation (Hino et al., 2005), suggesting that PKA stabilizes β-catenin and activates Wnt signalling. PKA mediated phosphorylation of β-catenin at Ser-552 and Ser-675 promotes transcriptional activity of β-catenin (Tcf/Lef transactivation) and it binding with transcriptional co-activator cAMP response element (CREB)-binding protein (Taurin et al., 2006). In support of these studies, we also found that D1 agonism positively regulates Wnt/β-catenin signalling by inhibiting the association of β-catenin destruction complex in 6-OHDA lesioned rats. Our data suggest that PKA mediated stabilization of β-catenin and Wnt signalling activation could be a secondary mechanism for D1 agonism induced DAergic neurogenesis in 6-OHDA lesioned rats.

Wnt/β-catenin signalling is an evolutionarily conserved regulator of organismal development that plays a crucial role for the maintenance

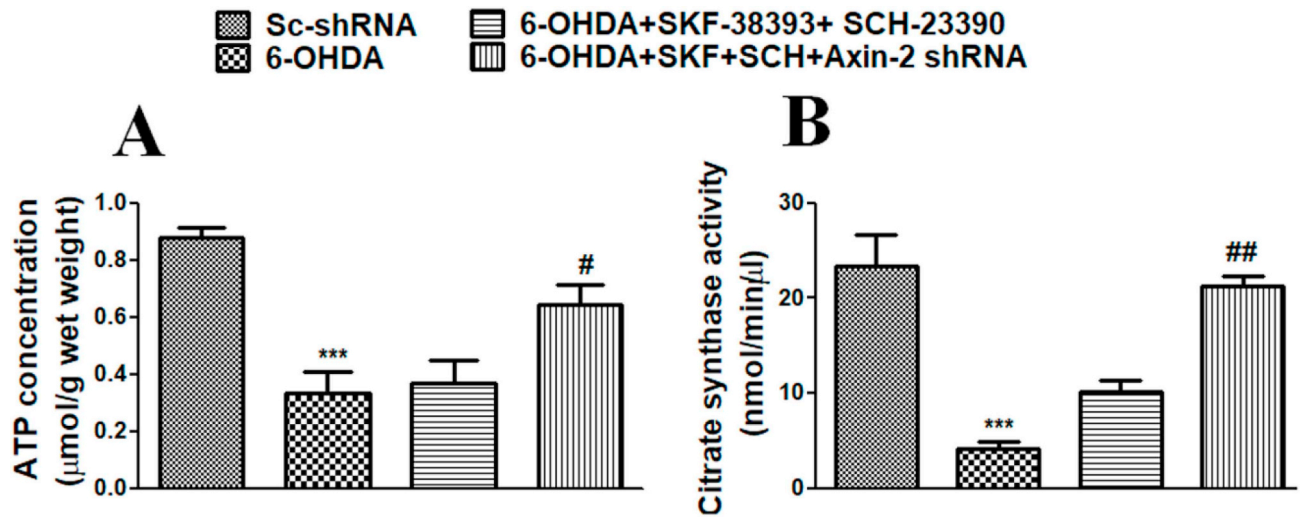

Fig. 14. Wnt/β-Catenin signaling activation restores D1 antagonist SCH-23390 induced reduction in mitochondrial functionality in SNpc region. **(A)** Bar graph show concentration of ATP in SNpc region **(B)** Bar graph show citrate synthase activity in SNpc. Data are expressed as mean ± SEM of n = 5 rats/group. Data were analyzed by one-way ANOVA followed by Bonferroni post hoc test (*P < 0.05, **P < 0.01, ***P < 0.001, $^{\#}$P < 0.05, $^{\#\#}$P < 0.01, $^{\#\#\#}$P < 0.001) * = scshRNAvs 6-OHDA + scshRNA, # = 6-OHDA + scshRNAvs 6-OHDA + Axin-2 shRNA.

and regulation of self-renewing and pluripotent capacity. 6-OHDA induced neurotoxicity has been reported to activate GSK-3β by hyperphosphorylation at Tyr-216 and inhibition of Ser-9 phosphorylation in cultured DAergic neurons (L'Episcopo et al., 2011). Moreover, pharmacological inhibition of Wnt/β-catenin signalling by recombinant DKK-1, a Wnt antagonist further aggravated the DAergic neuronal damage in SNpc of 6-OHDA induced rat model of PD-like phenotypes, suggesting a potential role of Wnt signalling in DAergic neurotoxicity (Dun et al., 2012). Consistent with these studies, we found that intra-MFB administration of 6-OHDA increased levels of Axin-2, APC and pTyr-216-GSK-3β which lead to persistent stabilization of the β-catenin destruction complex. Our data shows that 6-OHDA induced down-regulation of Wnt/β-catenin signalling by promoting the assembly of β-catenin destruction complex in the SNpc. In contrast, pharmacological inhibition of GSK-3β induced activation of Wnt/β-catenin signalling protect DAergic neurons against rotenone induced neurotoxicity in *in-vitro* by reducing apoptotic pathway and promoting Nurr-1, a transcription factor regulating DAergic development (Zhang et al., 2016a). Moreover, pharmacological inhibition of GSK-3β attenuate D1 receptor induced hyperactivity in mice (Miller et al., 2010). It has been shown that D2 receptors regulate GSK-3β and Akt via Dvl-3 in *in-vivo* and *in-vitro*, indicating a causal link between dopamine receptor and Wnt signalling. Therefore, it is reasonable to propose that D1 agonism induce activation of Wnt/β-catenin signalling in rat model of PD-like phenotype by inhibiting the components of β-catenin degradation complex in SNpc. Axin-2 is an important component of Wnt signalling pathways which suppress the signalling activity by enhancing phosphorylation and degradation of β-catenin, a central modulator protein of Wnt pathway (Jho et al., 2002). We further observed that shRNA mediated knockdown of Axin-2, a negative regulator of Wnt/β-catenin signalling facilitates mitochondrial functions, DAergic neuron differentiation and motor behaviour in D1 antagonist treated 6-OHDA lesioned rats by activation of Wnt/β-catenin signalling components. It has been reported that inducible expression of Axin-2 impaired neural tube patterning and cell placement in the midbrain of developing embryos by altering β-catenin levels (Yu et al., 2007). Induced overexpression of Wnt antagonist Dickkopf-1 (iDkk-1) in adult mice decrease the number of cortico-striatal glutamatergic synapses and dopamine D1 and D2 receptor clusters that lead to impairment in behavioural functions (Galli et al., 2014), further suggesting involvement of Wnt regulation and dopamine receptor in behavioural function and dopamine signalling. Interestingly, Axin expression in mitochondria reduces ATP levels and oxygen consumption rate in HeLa cells, suggesting a potential role of Axin in mitochondrial functioning (Shin et al., 2016). Therefore, we conclude that Axin-2 inhibition mediated activation of Wnt signalling enhance DAergic neurogenesis and improve motor behaviour by regulating mitochondrial functions in D1 antagonist treated 6-OHDA lesioned rats. Our study further, suggest a causal link between dopamine receptors mediated activation of Wnt signalling in rat model of PD-like phenotypes.

In conclusion, our current study provides evidence for stimulatory effects of dopamine on behavioural function, mitochondrial dynamics and DAergic neurogenesis. These effects are mediated by D1-like receptor activation and Wnt/β-catenin pathway. Targeting D1 like receptors in PD may help to enhance the behavioural functions, mitochondrial dynamics and DAergic neurogenesis, clearly pointing towards novel potential strategies to treat PD.

Disclosure statement

The authors declare that they have no conflict of interest.

Acknowledgement

This research work was funded by Council for Scientific and Industrial Research (CSIR), New Delhi, India, Network grants miND (BSC0115) to Dr. Shubha Shukla. Authors would like to thank Director of CSIR- Central Drug Research Institute, Lucknow, India for constant support during the study. Akanksha Mishra, Virendra Tiwari and Swati Chaturvedi are supported by a research fellowship from CSIR, New Delhi, India. Sonu Singh is supported by a research fellowship from Indian Council of Medical Research, New Delhi, India. The CDRI communication number is 9846.

Appendix A. Supplementary data

Supplementary data to this article can be found online at https://doi.org/10.1016/j.neuint.2019.104463.

References

Alam, Z.I., et al., 1997. Oxidative DNA damage in the parkinsonian brain: an apparent selective increase in 8-hydroxyguanine levels in substantia nigra. J. Neurochem. 69, 1196–1203.

Alexander, G.E., 2004. Biology of Parkinson's disease: pathogenesis and pathophysiology of a multisystem neurodegenerative disorder. Dialogues Clin. Neurosci. 6, 259–280.

Alimohamad, H., et al., 2005. Antipsychotics alter the protein expression levels of beta-catenin and GSK-3 in the rat medial prefrontal cortex and striatum. Biol. Psychiatry 57, 533–542.

Andersson, E.R., et al., 2008. Wnt5a regulates ventral midbrain morphogenesis and the development of A9-A10 dopaminergic cells in vivo. PLoS One 3 e3517.

Avila-Luna, A., et al., 2018. Dopamine D1 receptor activation maintains motor coordination and balance in rats. Metab. Brain Dis. 33, 99–105.

Bender, A., et al., 2006. High levels of mitochondrial DNA deletions in substantia nigra neurons in aging and Parkinson disease. Nat. Genet. 38, 515–517.

Brouillet, E., et al., 1995. Chronic mitochondrial energy impairment produces selective striatal degeneration and abnormal choreiform movements in primates. Proc. Natl. Acad. Sci. U. S. A. 92, 7105–7109.

Carvalho, M.M., et al., 2013. Behavioral characterization of the 6-hydroxidopamine model of Parkinson's disease and pharmacological rescuing of non-motor deficits. Mol. Neurodegener. 8, 14.

Cassarino, D.S., et al., 1998. Pramipexole reduces reactive oxygen species production in vivo and in vitro and inhibits the mitochondrial permeability transition produced by the parkinsonian neurotoxin methylpyridinium ion. J. Neurochem. 71, 295–301.

Castelo-Branco, G., et al., 2010. Delayed dopaminergic neuron differentiation in Lrp6 mutant mice. Dev. Dynam. 239, 211–221.

Castelo-Branco, G., et al., 2003. Differential regulation of midbrain dopaminergic neuron development by Wnt-1, Wnt-3a, and Wnt-5a. Proc. Natl. Acad. Sci. U. S. A. 100, 12747–12752.

Chen, S., et al., 2008. Dopamine inhibits mitochondrial motility in hippocampal neurons. PLoS One 3 e2804.

Dexter, D.T., et al., 1994. Increased levels of lipid hydroperoxides in the parkinsonian substantia nigra: an HPLC and ESR study. Mov. Disord. 9, 92–97.

Dolle, C., et al., 2016. Defective mitochondrial DNA homeostasis in the substantia nigra in Parkinson disease. Nat. Commun. 7, 13548.

Dun, Y., et al., 2012. Inhibition of the canonical Wnt pathway by Dickkopf-1 contributes to the neurodegeneration in 6-OHDA-lesioned rats. Neurosci. Lett. 525, 83–88.

Ekstrand, M.I., et al., 2007. Progressive parkinsonism in mice with respiratory-chain-deficient dopamine neurons. Proc. Natl. Acad. Sci. U. S. A. 104, 1325–1330.

Felten, D.L., et al., 1992. Chronic dietary pergolide preserves nigrostriatal neuronal integrity in aged-Fischer-344 rats. Neurobiol. Aging 13, 339–351.

Fiorentini, C., et al., 2006. Loss of synaptic D1 dopamine/N-methyl-D-aspartate glutamate receptor complexes in L-DOPA-induced dyskinesia in the rat. Mol. Pharmacol. 69, 805–812.

Floor, E., Wetzel, M.G., 1998. Increased protein oxidation in human substantia nigra pars compacta in comparison with basal ganglia and prefrontal cortex measured with an improved dinitrophenylhydrazine assay. J. Neurochem. 70, 268–275.

Fowler, C.J., Benedetti, M.S., 1983. The metabolism of dopamine by both forms of monoamine oxidase in the rat brain and its inhibition by cimoxatone. J. Neurochem. 40, 1534–1541.

Freundlieb, N., et al., 2006. Dopaminergic substantia nigra neurons project topographically organized to the subventricular zone and stimulate precursor cell proliferation in aged primates. J. Neurosci. 26, 2321–2325.

Galli, S., et al., 2014. Deficient Wnt signalling triggers striatal synaptic degeneration and impaired motor behaviour in adult mice. Nat. Commun. 5, 4992.

Gille, G., et al., 2002. Protection of dopaminergic neurons in primary culture by lisuride. J. Neural Transm. 109, 157–169.

Gnanalingham, K.K., et al., 1995. Selective dopamine antagonist pretreatment on the antiparkinsonian effects of benzazepine D1 dopamine agonists in rodent and primate models of Parkinson's disease–the differential effects of D1 dopamine antagonists in the primate. Psychopharmacology (Berl) 117, 403–412.

Hedlund, E., et al., 2016. Dopamine receptor antagonists enhance proliferation and neurogenesis of midbrain Lmx1a-expressing progenitors. Sci. Rep. 6, 26448.

Hisahara, S., Shimohama, S., 2011. Dopamine receptors and Parkinson's disease. Int. J. Med. Chem. 2011, 403039.

Hino, S., Tanji, C., Nakayama, K.I., Kikuchi, A., 2005. Phosphorylation of beta-catenin by cyclic AMP-dependent protein kinase stabilizes beta-catenin through inhibition of its ubiquitination. Mol. Cell. Biol. 25, 9063–9072.

Hoglinger, G.U., et al., 2004. Dopamine depletion impairs precursor cell proliferation in Parkinson disease. Nat. Neurosci. 7, 726–735.

Iida, M., et al., 1999. Dopamine D2 receptor-mediated antioxidant and neuroprotective effects of ropinirole, a dopamine agonist. Brain Res. 838, 51–59.

Ikebe, S., et al., 1990. Increase of deleted mitochondrial DNA in the striatum in Parkinson's disease and senescence. Biochem. Biophys. Res. Commun. 170, 1044–1048.

Jho, E.H., et al., 2002. Wnt/beta-catenin/Tcf signaling induces the transcription of Axin2, a negative regulator of the signaling pathway. Mol. Cell. Biol. 22, 1172–1183.

Johri, A., Beal, M.F., 2012. Mitochondrial dysfunction in neurodegenerative diseases. J. Pharmacol. Exp. Ther. 342, 619–630.

Joyce, J.N., et al., 2004. Low dose pramipexole is neuroprotective in the MPTP mouse model of Parkinson's disease, and downregulates the dopamine transporter via the D3 receptor. BMC Biol. 2, 22.

Keeney, P.M., et al., 2006. Parkinson's disease brain mitochondrial complex I has oxidatively damaged subunits and is functionally impaired and misassembled. J. Neurosci. 26, 5256–5264.

Kitamura, Y., et al., 1997. Inhibitory effects of talipexole and pramipexole on MPTP-induced dopamine reduction in the striatum of C57BL/6N mice. Jpn. J. Pharmacol. 74, 51–57.

Komiya, Y., Habas, R., 2008. Wnt signal transduction pathways. Organogenesis 4, 68–75.

Kraytsberg, Y., et al., 2006. Mitochondrial DNA deletions are abundant and cause functional impairment in aged human substantia nigra neurons. Nat. Genet. 38, 518–520.

Kupsch, A., et al., 2014. 6-Hydroxydopamine impairs mitochondrial function in the rat model of Parkinson's disease: respirometric, histological, and behavioral analyses. J. Neural Transm. 121, 1245–1257.

L'Episcopo, F., et al., 2011. A Wnt1 regulated Frizzled-1/beta-Catenin signaling pathway as a candidate regulatory circuit controlling mesencephalic dopaminergic neuron-astrocyte crosstalk: therapeutical relevance for neuron survival and neuroprotection. Mol. Neurodegener. 6, 49.

L'Episcopo, F., et al., 2014. Wnt/beta-catenin signaling is required to rescue midbrain dopaminergic progenitors and promote neurorepair in ageing mouse model of Parkinson's disease. Stem Cell. 32, 2147–2163.

Li, Y., et al., 2011. Knockdown of glycogen synthase kinase 3 beta attenuates 6-hydroxydopamine-induced apoptosis in SH-SY5Y cells. Neurosci. Lett. 487, 41–46.

Lie, D.C., et al., 2002. The adult substantia nigra contains progenitor cells with neurogenic potential. J. Neurosci. 22, 6639–6649.

Maurice, N., et al., 2004. D2 dopamine receptor-mediated modulation of voltage-dependent Na+ channels reduces autonomous activity in striatal cholinergic interneurons. J. Neurosci. 24, 10289–10301.

Medeiros, D.M., 2008. Assessing mitochondria biogenesis. Methods 46, 288–294.

Miller, J.S., et al., 2010. Inhibition of GSK3 attenuates dopamine D1 receptor agonist-induced hyperactivity in mice. Brain Res. Bull. 82, 184–187.

Min, C., et al., 2011. Novel regulatory mechanism of canonical Wnt signaling by dopamine D2 receptor through direct interaction with beta-catenin. Mol. Pharmacol. 80, 68–78.

Ming, G.L., Song, H., 2011. Adult neurogenesis in the mammalian brain: significant answers and significant questions. Neuron 70, 687–702.

Mishra, A., et al., 2018. Physiological and functional basis of dopamine receptors and their role in neurogenesis: possible implication for Parkinson's disease. J. Exp. Neurosci. 12 1179069518779829.

Mishra, A., et al., 2019. Dopamine D1 receptor activation improves adult hippocampal neurogenesis and exerts anxiolytic and antidepressant-like effect via activation of Wnt/beta-catenin pathways in rat model of Parkinson's disease. Neurochem. Int. 122, 170–186.

Morozov, Y.I., et al., 2014. A novel intermediate in transcription initiation by human mitochondrial RNA polymerase. Nucleic Acids Res. 42, 3884–3893.

Neve, K.A., Seamans, J.K., Trantham-Davidson, H., 2004. Dopamine receptor signaling. J. Recept. Signal Transduct. Res. 24, 165–205.

Parkinson, G.M., et al., 2014. Increased mitochondrial DNA deletions in substantia nigra dopamine neurons of the aged rat. Curr. Aging Sci. 7, 155–160.

Pyle, A., et al., 2016. Reduced mitochondrial DNA copy number is a biomarker of Parkinson's disease. Neurobiol. Aging 38 216 e7-216 e10.

Ramachandran, A., et al., 2017. Human mitochondrial transcription factors TFAM and TFB2M work synergistically in promoter melting during transcription initiation. Nucleic Acids Res. 45, 861–874.

Reddy, S.S., et al., 2018. Cilostazol ameliorates heart failure with preserved ejection fraction and diastolic dysfunction in obese and non-obese hypertensive mice. J. Mol. Cell. Cardiol. 123, 46–57.

Robertson, G.S., et al., 1991. Dopaminergic grafts in the striatum reduce D1 but not D2 receptor-mediated rotation in 6-OHDA-lesioned rats. Brain Res. 539, 304–311.

Salvi, R., et al., 2016. Distinct effects of chronic dopaminergic stimulation on hippocampal neurogenesis and striatal Doublecortin expression in adult mice. Front. Neurosci. 10, 77.

Scarpulla, R.C., 2008. Transcriptional paradigms in mammalian mitochondrial biogenesis and function. Physiol. Rev. 88, 611–638.

Schapira, A.H., 1999. Mitochondrial involvement in Parkinson's disease, Huntington's disease, hereditary spastic paraplegia and Friedreich's ataxia. Biochim. Biophys. Acta 1410, 159–170.

Schapira, A.H., et al., 1989. Mitochondrial complex I deficiency in Parkinson's disease. Lancet 1, 1269.

Scholpa, N.E., et al., 2018. 5-HT1F receptor-mediated mitochondrial biogenesis for the treatment of Parkinson's disease. Br. J. Pharmacol. 175, 348–358.

Shin, J.H., et al., 2016. Axin is expressed in mitochondria and suppresses mitochondrial ATP synthesis in HeLa cells. Exp. Cell Res. 340, 12–21.

Singh, S., et al., 2018a. Axin-2 knockdown promote mitochondrial biogenesis and dopaminergic neurogenesis by regulating Wnt/beta-catenin signaling in rat model of Parkinson's disease. Free Radic. Biol. Med. 129, 73–87.

Singh, S., et al., 2018b. Acetyl-l-carnitine via upegulating dopamine D1 receptor and attenuating microglial activation prevents neuronal loss and improves memory functions in parkinsonian rats. Mol. Neurobiol. 55, 583–602.

Singh, S., et al., 2017. MK-801 (dizocilpine) regulates Multiple steps of adult hippocampal neurogenesis and alters psychological symptoms via Wnt/beta-catenin signaling in parkinsonian rats. ACS Chem. Neurosci. 8, 592–605.

Thomas, K.R., Capecchi, M.R., 1990. Targeted disruption of the murine int-1 proto-oncogene resulting in severe abnormalities in midbrain and cerebellar development. Nature 346, 847–850.

Thomas, R.R., et al., 2012. Impaired complex-I mitochondrial biogenesis in Parkinson disease frontal cortex. J. Parkinson's Dis. 2, 67–76.

Tozzi, A., et al., 2018. Dopamine D2 receptor-mediated neuroprotection in a G2019S Lrrk2 genetic model of Parkinson's disease. Cell Death Dis. 9, 204.

Taurin, S., Sandbo, N., Qin, Y., Browning, D., Dulin, N.O., 2006. Phosphorylation of beta-

catenin by cyclic AMP-dependent protein kinase. J. Biol. Chem. 281, 9971–9976.
Uittenbogaard, M., Chiaramello, A., 2014. Mitochondrial biogenesis: a therapeutic target for neurodevelopmental disorders and neurodegenerative diseases. Curr. Pharmaceut. Des. 20, 5574–5593.
Undieh, A.S., 2010. Pharmacology of signaling induced by dopamine D(1)-like receptor activation. Pharmacol. Ther. 128, 37–60.
van der Kooij, M.A., et al., 2018. Diazepam actions in the VTA enhance social dominance and mitochondrial function in the nucleus accumbens by activation of dopamine D1 receptors. Mol. Psychiatry 23, 569–578.
Van Kampen, J.M., Robertson, H.A., 2005. A possible role for dopamine D3 receptor stimulation in the induction of neurogenesis in the adult rat substantia nigra. Neuroscience 136, 381–386.
Winner, B., et al., 2009. Dopamine receptor activation promotes adult neurogenesis in an acute Parkinson model. Exp. Neurol. 219, 543–552.
Xi, Y., et al., 2018. MitoQ protects dopaminergic neurons in a 6-OHDA induced PD model by enhancing Mfn2-dependent mitochondrial fusion via activation of PGC-1 alpha. Biochim. Biophys. Acta (BBA) - Mol. Basis Dis. 1864, 2859–2870.
Yu, H.M., et al., 2007. Impaired neural development caused by inducible expression of Axin in transgenic mice. Mech. Dev. 124, 146–156.
Zhang, L., et al., 2016a. Enhancing beta-catenin activity via GSK3beta inhibition protects PC12 cells against rotenone toxicity through Nurr1 induction. PLoS One 11 e0152931.
Zhang, T., et al., 2016b. MPTP impairs dopamine D1 receptor-mediated survival of newborn neurons in ventral Hippocampus to cause depressive-like behaviors in adult mice. Front. Mol. Neurosci. 9, 101.
Zhao, M., et al., 2003. Evidence for neurogenesis in the adult mammalian substantia nigra. Proc. Natl. Acad. Sci. U. S. A. 100, 7925–7930.
Zou, L., et al., 2000. Pramipexole inhibits lipid peroxidation and reduces injury in the substantia nigra induced by the dopaminergic neurotoxin 1-methyl-4-phenyl-1,2,3,6-tetrahydropyridine in C57BL/6 mice. Neurosci. Lett. 281, 167–170.